

**INTEGRATION AND QUANTIFICATION OF UNCERTAINTY OF
VOLUMETRIC AND MATERIAL BALANCE ANALYSES USING A BAYESIAN
FRAMEWORK**

A Thesis

by

CHILE OGELE

Submitted to the Office of Graduate Studies of
Texas A&M University
in partial fulfillment of the requirements for the degree of

MASTER OF SCIENCE

August 2005

Major Subject: Petroleum Engineering

**INTEGRATION AND QUANTIFICATION OF UNCERTAINTY OF
VOLUMETRIC AND MATERIAL BALANCE ANALYSES USING A BAYESIAN
FRAMEWORK**

A Thesis

by

CHILE OGELE

Submitted to the Office of Graduate Studies of
Texas A&M University
in partial fulfillment of the requirements for the degree of

MASTER OF SCIENCE

Approved by

Chair of Committee,
Committee Members,

Head of Department,

Duane A. McVay
W. John Lee
Wayne M. Ahr
Stephen A. Holditch

August 2005

Major Subject: Petroleum Engineering

ABSTRACT

Integration and Quantification of Uncertainty of Volumetric and Material Balance

Analyses Using a Bayesian Framework. (August 2005)

Chile Ogele, B.Eng.; M.Eng., University of Port Harcourt, Nigeria

Chair of Advisory Committee: Dr. Duane A. McVay

Estimating original hydrocarbons in place (OHIP) in a reservoir is fundamentally important to estimating reserves and potential profitability. Quantifying the uncertainties in OHIP estimates can improve reservoir development and investment decision-making for individual reservoirs and can lead to improved portfolio performance. Two traditional methods for estimating OHIP are volumetric and material balance methods. Probabilistic estimates of OHIP are commonly generated prior to significant production from a reservoir by combining volumetric analysis with Monte Carlo methods. Material balance is routinely used to analyze reservoir performance and estimate OHIP. Although material balance has uncertainties due to errors in pressure and other parameters, probabilistic estimates are seldom done.

In this thesis I use a Bayesian formulation to integrate volumetric and material balance analyses and to quantify uncertainty in the combined OHIP estimates. Specifically, I apply Bayes' rule to the Havlena and Odeh material balance equation to estimate original oil in place, N , and relative gas-cap size, m , for a gas-cap drive oil reservoir. The paper considers uncertainty and correlation in the volumetric estimates of N and m (reflected in the prior probability distribution), as well as uncertainty in the pressure data (reflected in the likelihood distribution). Approximation of the covariance of the posterior distribution allows quantification of uncertainty in the estimates of N and m resulting from the combined volumetric and material balance analyses.

Several example applications to illustrate the value of this integrated approach are presented. Material balance data reduce the uncertainty in the volumetric estimate, and the volumetric data reduce the considerable non-uniqueness of the material balance solution, resulting in more accurate OHIP estimates than from the separate analyses. One of the advantages over reservoir simulation is that, with the smaller number of parameters in this approach, we can easily sample the entire posterior distribution, resulting in more complete quantification of uncertainty. The approach can also detect underestimation of uncertainty in either volumetric data or material balance data, indicated by insufficient overlap of the prior and likelihood distributions. When this occurs, the volumetric and material balance analyses should be revisited and the uncertainties of each reevaluated.

DEDICATION

I wish to dedicate my thesis:

To God almighty, for his guidance and blessing over my life,
To my true love, Mercy
for all your support and especially for your unconditional love
and
To my boys, Chidubem, Chimela and Christopher
who are the special gift in my life, I love you all.

ACKNOWLEDGMENTS

I wish to express my sincere gratitude and appreciation to:

Dr. Duane A. McVay, chair of my advisory committee, for his excellent supervision and support throughout my research. It was great to work with him.

Dr. W. John Lee, member of my committee, for his enthusiastic and active participation during my investigation. It was an honor and a great experience.

Dr. Wayne M. Ahr, member of my committee, for his involvement in my research. I enjoyed your carbonate class.

Dr. Ahmed M. Daoud, for his initial work on the Bayesian code. Thank you for all the computer programming support you gave me.

Dr. Blasingame, for his wise words and unconditional advises. Thank you so much.

Ms. Weatherford, for all the technical writing skill you impacted in me. Thank you.

Chevron Nigeria Limited, for sponsoring my M.S. program at Texas A&M University. Thank you for giving me the opportunity to improve my knowledge in Petroleum Engineering.

Finally, I want to express my gratitude and appreciation to all my colleagues at Texas A&M University: Igho, Amara Okeke, Kabiru Abubakar, Dayo Oyerinde, Yuhong Wang, Jay Holmes and many more too numerous to list here.

TABLE OF CONTENTS

		Page
ABSTRACT		iii
DEDICATION		v
ACKNOWLEDGMENTS		vi
TABLE OF CONTENTS		vii
LIST OF FIGURES		ix
LIST OF TABLES		xi
CHAPTER		
I	INTRODUCTION	1
	Research Background	1
	Objectives	5
	General Approach	5
II	METHODOLOGY	6
	Bayes' Theory for Combining Volumetric and Material Balance Analyses	6
	Quantification of Uncertainties in Posterior N and m Values	9
III	APPLICATION CASES AND RESULTS	13
	Example 1: Gas-cap Oil Reservoir Reported by Dake	13
	Case 1: Large Uncertainty in Prior and Small Uncertainty in Pressure Data	13
	Case 2: Large Uncertainty in Both Prior and Pressure Data	19
	Case 3: Large Uncertainty in Prior With 50 psia Pressure Data Uncertainty	23
	Case 4: Situation With Small Overlap Between Prior and Likelihood	25
	Case 5: Situations With Negligible Overlap Between Prior and Likelihood	27
	Implications for Higher-Dimensional Problems	31
	Example 2: Synthetic Gas-cap Oil Reservoir Presented by Walsh	32
IV	CONCLUSIONS	39
NOMENCLATURE		40
REFERENCES		41

	Page
APPENDIX A: BAYESIAN MAIN CODE	44
APPENDIX B: MODIFIED SUBROUTINE FOR EXAMPLE 2	61
VITA	63

LIST OF FIGURES

FIGURE		Page
3.1	Prior distribution of N and m for case with large uncertainty in the prior for $\rho=0$	15
3.2	Prior distribution of N and m for case with large uncertainty in the prior for $\rho=-0.6$	16
3.3	Increasing magnitude of parameter correlation demarcates smaller region in space.....	16
3.4	Likelihood distribution of N and m for case with small uncertainty in pressure data.....	17
3.5	Posterior distribution of N and m for case with small uncertainty in pressure data for $\rho=0$	18
3.6	Composite plots show that the posterior distributions lie within the prior and likelihood distributions	18
3.7	Likelihood distribution for case with large pressure data uncertainty shows considerable non-uniqueness in material balance solution	20
3.8	Pressure history match for different N,m solutions (Fig. 4.7) show non-uniqueness of material balance solution	21
3.9	Posterior distributions for cases with large prior and large data uncertainty	22
3.10	Composite plot for case with large prior and large data uncertainty	22
3.11	Composite plot for cases with large prior and 50 psia pressure data uncertainty	24
3.12	Increasing magnitude of parameter correlation reduces uncertainty in posterior estimates of N and m	25
3.13	Composite plot for case with small overlap in prior and likelihood shows reconciliation of volumetric and material balance analyses.....	26
3.14	Composite plot for case with large uncertainty in both prior and data, and negligible overlap between prior and likelihood distributions	27
3.15	Composite plot for case with small prior uncertainty, large data uncertainty, and negligible overlap between prior and likelihood	29
3.16	Composite plot for case with small uncertainty in both prior and data, and negligible overlap between prior and likelihood distributions	30

FIGURE		Page
3.17	Pre-posterior increases as prior and likelihood overlap significantly	33
3.18	Composite plot for Example 2 with 10 psia error in pressure data	36
3.19	Composite plot for Example 2 with 50 psia error in pressure data	37
3.20	Composite plot for Example 2 with 100 psia error in pressure data	37

LIST OF TABLES

TABLE		Page
3.1	Pressure, Cumulative Production, and PVT Data for Example 1	14
3.2	Summary of Results for Case 1	19
3.3	Summary of Results for Case 2	23
3.4	Summary of Results for Case 3	24
3.5	Summary of Results for Case 5a	28
3.6	Reservoir Properties for Example 2	34
3.7	Black-Oil PVT Properties for Example 2	34
3.8	Cumulative Oil and Gas Production History for Example 2	35
3.9	Summary of Volumetric Analysis	35
3.10	Summary of Results for Example 2	38

CHAPTER I

INTRODUCTION

Research Background

The estimation of original hydrocarbons in place (OHIP) in a reservoir is one of the oldest and, still, most important problems in reservoir engineering. Estimating OHIP in a reservoir is fundamentally important to estimating reserves and potential profitability. We have long known that our estimates of OHIP possess uncertainty¹⁻³ due to data inaccuracies and scarcity of data. Quantifying the uncertainties in OHIP estimates can improve reservoir development and investment decision-making for individual reservoirs and can lead to improved portfolio performance.⁴ The general question I address in this thesis is: Given all the various types of reservoir data available, how do we best estimate OHIP and how do we quantify the uncertainty inherent in this estimate?

Two traditional methods for estimating OHIP are volumetric and material balance methods.^{5,6} Volumetric methods are based on static reservoir properties, such as porosity, net thickness and initial saturation distributions. Since they can be applied prior to production from the reservoir, volumetric methods are often the only source of OHIP values available in making the large investment decisions required early in the life of a reservoir. Given the often large uncertainty due to paucity of well data early in the reservoir life, it is common to quantify the uncertainty of volumetric estimates of OHIP using statistical methods such as Confidence Interval⁷ and Monte Carlo analysis.^{8,9}

Material balance is routinely used to analyze reservoir performance data and estimate OHIP. The material balance method requires pressure and production data and, thus, can be applied only after the reservoir has produced for a significant period of time. The advantages of material balance methods are (1) we can determine drive mechanism in

This thesis follows the style of the *Society of Petroleum Engineers Journal*.

additional to OHIP, (2) no geological model is required, and (3) we can solve for OHIP (and sometimes other parameters) directly from performance data. Primary sources of uncertainty in material balance analyses are incomplete or inaccurate production data and inaccuracies in determining an accurate average pressure trend, particularly in low-permeability or heterogeneous reservoirs. Although these uncertainties have been long recognized, since material balance methods are based on observed performance data, they are often considered more accurate than volumetric methods. Thus, it is uncommon to formally quantify the uncertainty in material balance estimates of OHIP, although there have been some attempts.¹⁰⁻¹³

McEwen¹⁰ presented a technique for material balance calculations with water influx in the presence of uncertainty in pressures. He introduced a major change by limiting the least-square line-fitting to yield only one constant, OHIP. His approach did not fully quantify the uncertainty in the OHIP estimate. Later, Fair¹¹ discussed the application of a method to perform regression analysis of the material balance equations. He expressed the uncertainty in the OHIP estimate in terms of a confidence interval. Wang and Hwan¹² used a statistical approach to investigate and provide explanation for the uncertainties in material balance calculation for various types of reservoirs. They suggested the use of a reservoir voidage replacement plot as a good measure to quantify the uncertainty level. None of these attempts integrates data from volumetric analysis.

Volumetric and material balance methods provide independent estimates of OHIP, since they rely on different data sets: static data for volumetric methods and dynamic data for material balance methods. Both volumetric and material balance analyses individually have valid justification for utilization. When used jointly, they can provide even greater insight into estimates of OHIP. However, traditional material balance methods are often skipped in reservoir studies today, since reservoir simulation has become the preferred mechanism for integrating static and dynamic data. Omitting material balance analysis is often unwise because this analysis still has considerable value, particularly as a precursor

to reservoir simulation studies.¹⁴ Material balance analysis can help narrow the range of the many parameters, including OHIP that can be adjusted during simulation.¹⁵

Comparing and reconciling estimates from both methods can lead to a more accurate estimate of OHIP, as well as a feel for the uncertainty in the estimate. In the absence of reservoir simulation, this reconciliation has usually been done informally. According to Dake,¹⁴ "Material balance used to be a valuable point of contact between engineers and geologists. If the material balance OHIP turned out to be, say, 10% lower than the volumetric estimate they would get together to try and figure out why this disparity existed..." Some have attempted to reconcile both estimates by using a filtered Monte Carlo method,¹⁶ which screens input parameters to volumetric analysis and accepts only those sets that lead to a consistent estimate of OHIP. This approach will likely not fully quantify the uncertainty in the OHIP since it eliminates some sets of input parameters. The authors assumed that the estimate of OHIP from material balance is the more accurate. A better approach to solve the problem is to integrate both analyses under a single framework.

In recent years, Bayesian formalism¹⁷⁻¹⁹ has been introduced as a framework for reconciling static data and dynamic data in reservoir simulation. Reservoir simulation has become a convenient mechanism for combining volumetric and material balance analyses, since it incorporates both static and dynamic data. Unlike material balance methods, OHIP and other reservoir parameters cannot be solved for directly. Reservoir simulation requires the solution of an inverse problem, in which the reservoir description and OHIP are determined by history matching observed performance data. It is through history matching that volumetric and material balance estimates of OHIP are reconciled.

Early on, reservoir simulation was most often used deterministically to generate most-likely forecasts of reservoir performance. When attempts to quantify uncertainty were made, it was often done by making perturbation runs after the history match was

complete.²⁰ In Bayesian methods, prior probability distributions of reservoir parameters available from static data are conditioned to observed dynamic data to yield posterior probability distributions of the reservoir parameters, which are then sampled to quantify the uncertainty of production forecasts. While Bayesian methods can be quite helpful, the large number of parameters present in typical reservoir simulation models presents several difficulties. First, since the parameter space is usually many-dimensional and not easily visualized, it may be difficult to fully comprehend parameter interactions. Due to the computational burden, it is usually necessary to reduce the number of parameters, which can introduce bias and result in an underestimation of the uncertainty in the production forecasts. Even with a reduction in the number of parameters, in most cases the number of parameters is still large enough that it is virtually impossible to fully sample the posterior distribution, which can result in either underestimation or overestimation of the uncertainty. Thus, while we may be able to model the reservoir with greater resolution using reservoir simulation, we may be limited in our ability to fully quantify the uncertainty of results from reservoir simulation models.

Since material balance methods involve many fewer parameters than reservoir simulation, this suggests that there may be value in application of Bayesian methods to combine volumetric and material balance analyses. Literature search reveals only one previous application of Bayesian methods to material balance analysis. Hwan²¹ combined a material balance program with a Bayesian-based history matching program to improve the accuracy of material balance results. However, he did not quantify the uncertainty of the resulting parameters. The specific question addressed in this research is whether Bayesian methods can be used to integrate volumetric and material balance estimates of OHIP and to quantify the uncertainties in these estimates.

Objectives

The goals of this research are as follows:

1. Apply Bayesian formalism to integrate volumetric and material balance analyses to better estimate OHIP and quantify uncertainty. Test the framework using data for gas-cap oil reservoirs reported in the literature.
2. Investigate the effect of correlation between parameters of the prior distribution on the combined OHIP estimate.

General Approach

In the remainder of this thesis I first provide a mathematical background of Bayes' theory as applied to integration of volumetric and material balance OHIP estimates using the Havlena and Odeh formulation.²² Second, I outline the approach used to quantify uncertainties in original oil in place, N , and ratio of gas-cap volume to oil volume, m . Finally, I demonstrate the concept using two field examples reported in the literature.

CHAPTER II METHODOLOGY

Bayes' Theory for Combining Volumetric and Material Balance Analyses

Bayes' theorem quantifies how new information can be used to revise the probabilities associated with various states of nature. The theory is the basis of the framework for combining the prior probability distribution of OHIP obtained from volumetric analysis with the likelihood distribution from material balance analysis of pressure and production data for gas-cap drive oil reservoirs. The resulting improved probability distribution for OHIP, the posterior distribution, incorporates uncertainties from the volumetric analysis as well as uncertainties from the material balance analysis due to errors in observed pressure data. Bayes' rule^{23,24} is as follows:

$$f(\mathbf{x} | \mathbf{d}^{\text{obs}}) = f(\mathbf{x}) \cdot \frac{f(\mathbf{d}^{\text{obs}} | \mathbf{x})}{\int_{-\infty}^{+\infty} f(\mathbf{d}^{\text{obs}} | \mathbf{x})f(\mathbf{x})d\mathbf{x}} \dots\dots\dots (2.1)$$

where \mathbf{x} is the vector of model parameters, \mathbf{d}^{obs} is the vector of observed pressure data, $f(\mathbf{x})$ is the prior probability distribution function of the model parameters, $f(\mathbf{d}^{\text{obs}} | \mathbf{x})$ is the likelihood probability distribution of the observed pressure data given parameters \mathbf{x} , and $f(\mathbf{x} | \mathbf{d}^{\text{obs}})$ is the posterior probability distribution of the model parameters given the observed data. The posterior is a conditional probability. The denominator in Eq. 2.1 is the marginal probability and is also called the pre-posterior.^{25,26} The pre-posterior is a constant value that normalizes the posterior distribution. Consequently, removing it from Eq. 2.1 will not affect the shape of the posterior distribution.

Assuming the uncertainties in the parameters, $f(\mathbf{x})$, and the model plus measured data, $f(\mathbf{d}^{\text{obs}} | \mathbf{x})$, follow Gaussian distributions, $f(\mathbf{x})$ and $f(\mathbf{d}^{\text{obs}} | \mathbf{x})$ can be written as:

$$f(\mathbf{x}) = \frac{1}{(2\pi)^{n_x/2} [\det(\mathbf{C}_x)]^{1/2}} \exp\left\{-\frac{1}{2}\left[(\mathbf{x} - \mathbf{x}_{\text{prior}})^T \mathbf{C}_x^{-1} (\mathbf{x} - \mathbf{x}_{\text{prior}})\right]\right\} \dots\dots\dots (2.2)$$

$$f(\mathbf{d}^{\text{obs}}|\mathbf{x}) = \frac{1}{(2\pi)^{n_d/2} [\det(\mathbf{C}_D)]^{1/2}} \exp\left\{-\frac{1}{2}\left[(g(\mathbf{x}) - \mathbf{d}^{\text{obs}})^T \mathbf{C}_D^{-1} (g(\mathbf{x}) - \mathbf{d}^{\text{obs}})\right]\right\} \dots\dots (2.3)$$

where n_x is the number of model parameters, n_d is the number of measured (observed) data points, $\mathbf{x}_{\text{prior}}$ is the vector of mean, or most likely, values of the model parameters from the prior distribution, \mathbf{C}_x is the prior parameter covariance matrix, which quantifies the prior uncertainties in the model parameters, $g(\mathbf{x})$ is the forward model as a function of the model parameters, \mathbf{C}_D is the data covariance matrix, which quantifies the uncertainties in the measured data, and $\det()$ is the determinant.

Eq. 2.2 is the multi-dimensional Gaussian probability distribution of the uncertainties in the model parameters, the prior distribution. This equation assumes that the prior distribution is multi-variate and normally distributed and, therefore, can be represented by the means and covariance of the variables. Eq. 2.3 is the multi-dimensional Gaussian probability distribution of the combined uncertainties in the measured data and the theoretical forward model, the likelihood distribution. Assuming the uncertainties in the forward model are negligible, Eq. 2.3 can be considered the uncertainties related only to the measured data. Of particular interest is the maximum likelihood (ML) value. This is the solution corresponding to the mode, or maximum value, of the likelihood probability distribution function, i.e., the set of parameters that results in the best match of the measured data. The ML is the solution that would be obtained if the material balance model was solved backward directly for the parameters assuming no error in the measured data.

Substituting Eqs. 2.2 and 2.3 into Eq. 2.1 yields the posterior distribution, which quantifies the uncertainty in the model parameters given both the prior information and the measured data. The mode of the posterior distribution function is the *maximum a posteriori* (MAP) solution. This is the most probable set of parameter values considering both the prior information and the measured data.

The forward model, $g(\mathbf{x})$, is the material balance equation for oil with original gas cap, expressing pressure implicitly as a function of N and m . Using the formulation by Havlena and Odeh,²²

$$F = N(E_o + m E_g) \dots\dots\dots (2.4)$$

where

$$E_o = (B_o - B_{oi}) + (R_{si} - R_s)B_g \dots\dots\dots (2.5)$$

$$E_g = B_{oi} \left(\frac{B_g}{B_{gi}} - 1 \right) \dots\dots\dots (2.6)$$

$$F = N_p (B_o + (R_p - R_s)B_g) \dots\dots\dots (2.7)$$

Note that, in Eq. 2.4, pressure is implicit since B_o , B_g , and R_s are pressure dependent. Eq. 2.4 is solved iteratively for pressure given N and m using the Gauss-Newton method. The formulation used in the iteration process is written as

$$f(p) = F - N(E_o + m E_g) = 0 \dots\dots\dots (2.8)$$

The parameters \mathbf{x} and \mathbf{x}_{prior} in Eq. 2.2 are defined as follows:

$$\mathbf{x} = \begin{bmatrix} N \\ m \end{bmatrix}, \quad \mathbf{x}_{prior} = \begin{bmatrix} N_{prior} \\ m_{prior} \end{bmatrix}$$

where N_{prior} and m_{prior} are the means, or most likely, values of N and m , respectively, obtained from volumetric analysis. The covariance matrix, which quantifies the uncertainties in N and m from volumetric analysis, in Eq. 2.2 is as follows:

$$\mathbf{C}_x = \begin{bmatrix} \sigma_N^2 & \rho\sigma_N\sigma_m \\ \rho\sigma_N\sigma_m & \sigma_m^2 \end{bmatrix} \dots\dots\dots (2.9)$$

where σ_N and σ_m are the standard deviations of prior N and m , respectively, and ρ is the correlation coefficient between N and m . The correlation coefficient between N and m should be negative, since N and m should normally be inversely related as they trade off due to uncertainty in gas-oil contact elevation. In Chapter III, I investigate the effect of correlation²⁷ by assuming correlation coefficients ranging from -0.90 to zero.

If ρ equals zero, Eq. 2.9 reduces to:

$$\mathbf{C}_x = \begin{bmatrix} \sigma_N^2 & 0 \\ 0 & \sigma_m^2 \end{bmatrix} \dots\dots\dots (2.10)$$

Recall that \mathbf{d}^{obs} in Eq. 2.3 is the vector of observed pressure data points and can be written as:

$$\mathbf{d}^{\text{obs}} = [P_1^{\text{obs}} \quad P_2^{\text{obs}} \quad \dots \quad P_{nd}^{\text{obs}}]^T \dots\dots\dots (2.11)$$

$\mathbf{g}(\mathbf{x})$ in Eq. 2.3 is the vector of pressures calculated iteratively from Eqs. 2.4-2.7:

$$\mathbf{g}(\mathbf{x}) = [P_1^{\text{calc}} \quad P_2^{\text{calc}} \quad \dots \quad P_{nd}^{\text{calc}}]^T \dots\dots\dots (2.12)$$

Assuming that the errors in the measured pressure data points are uncorrelated, the data covariance matrix, \mathbf{C}_D , in Eq. 2.3 is:

$$\mathbf{C}_D = \begin{bmatrix} \sigma_{p_1}^2 & 0 & 0 & 0 \\ 0 & \sigma_{p_2}^2 & & 0 \\ 0 & & \sigma_{p_3}^2 & 0 \\ 0 & 0 & 0 & \sigma_{p_{nd}}^2 \end{bmatrix}_{nd \times nd} \dots\dots\dots (2.13)$$

where σ_{p_i} , $i=1,nd$ are the standard deviations of the pressure measurements. If the standard deviations at all measured points are equal, then Eq. 2.13 can be written as:

$$\mathbf{C}_D = \begin{bmatrix} \sigma_p^2 & 0 & 0 & 0 \\ 0 & \sigma_p^2 & & 0 \\ 0 & & \sigma_p^2 & 0 \\ 0 & 0 & 0 & \sigma_p^2 \end{bmatrix}_{nd \times nd} \dots\dots\dots (2.14)$$

Eq. 2.1 yields the posterior distribution, a 2D probability distribution that quantifies uncertainties in N and m considering information from both volumetric and material balance analyses. The posterior distribution is generally non-Gaussian.

Quantification of Uncertainties in Posterior N and m Values

The posterior distribution, which is a multidimensional, contains the most complete information regarding the uncertainties in N and m . However, multidimensional

probability distributions are often difficult to comprehend, particularly when non-Gaussian. Therefore, it is useful to represent the uncertainties in a form that is more easily understood and utilized by decision makers. One such representation is the covariance of the posterior distribution. The posterior covariance matrix gives an indication of the uncertainties associated with the model parameters. It can be approximated at the *maximum a posteriori* (MAP) value. The MAP is the mode of the posterior distribution, which is considered the most probable parameter set.

The covariance can be calculated by analytical or numerical methods. In the analytical method, the observed data and model parameters are assumed to be quasi-linear around the MAP estimate. According to Tarantola²³ and Duijndam,²⁸ the covariance of the posterior distribution is then related to the covariance of the observed data and prior by the following:

$$\mathbf{C}_{x(\text{posterior})} = \left(\mathbf{G}_{\text{MAP}}^T \cdot \mathbf{C}_D^{-1} \cdot \mathbf{G}_{\text{MAP}} + \mathbf{C}_{x(\text{prior})}^{-1} \right)^{-1} \dots\dots\dots (2.15)$$

Where $\mathbf{C}_{x(\text{posterior})}$ is the covariance matrix approximated at the MAP, \mathbf{C}_D is the data covariance matrix, $\mathbf{C}_{x(\text{prior})}$ is the prior covariance matrix and \mathbf{G}_{MAP} is the sensitivity matrix at the MAP of the forward model with respect to N and m , evaluated as follows:

$$\mathbf{G}_{\text{MAP}} = \begin{bmatrix} \frac{\partial P_1}{\partial N} & \frac{\partial P_2}{\partial N} & \dots & \dots & \frac{\partial P_{nd}}{\partial N} \\ \frac{\partial P_1}{\partial m} & \frac{\partial P_2}{\partial m} & \dots & \dots & \frac{\partial P_{nd}}{\partial m} \end{bmatrix}^T \dots\dots\dots (2.16)$$

The numerical method uses basic laws of the joint probability function for discrete random variables²⁹ to calculate the covariance matrix for the posterior probability distribution:

$$\mathbf{C}_{x(\text{posterior})} = \begin{bmatrix} \text{cov}(N, N) & \text{cov}(N, m) \\ \text{cov}(m, N) & \text{cov}(m, m) \end{bmatrix} \dots\dots\dots (2.17)$$

The entries can be calculated using the expectation rules for the joint probability function. For example,

$$\text{cov}(N, N) = E(N^2) - E(N) \cdot E(N) \dots\dots\dots (2.18)$$

and

$$E(N^2) = \sum_N \sum_m N^2 \cdot f(N, m | \mathbf{d}^{\text{obs}}) \dots\dots\dots (2.19)$$

Similarly,

$$\text{cov}(N, m) = \text{cov}(m, N) = E(N \cdot m) - E(N) \cdot E(m) \dots\dots\dots (2.20)$$

and

$$E(N \cdot m) = \sum_N \sum_m N \cdot m \cdot f(N, m | \mathbf{d}^{\text{obs}}) \dots\dots\dots (2.21)$$

where $f(N, m | \mathbf{d}^{\text{obs}})$ is the posterior joint probability function obtained from Eq. 2.1.

The uncertainties can further be simplified by examining the standard deviations of N and m individually. The standard deviations are obtained by taking the square roots of the variances along the diagonal of the covariance matrix. Furthermore, these values can be compared with the diagonal elements of the prior covariance matrix to determine the extent to which the volumetric uncertainties in N and m have been reduced by conditioning to material balance data.

The procedure is summarized as follows:

1. Create a joint prior probability function of N and m using the mean and covariance matrix obtained from volumetric analysis assuming Gaussian distribution of the variables.
2. Calculate a likelihood function using the observed pressures and the Havlena and Odeh material balance model that predicts pressure for a given set of N and m .
3. Use Bayes' rule to combine the prior distribution and the likelihood function to obtain the posterior distribution.
4. Select the MAP, or mode, of the posterior distribution as the most probable (N, m) set.

5. Determine the uncertainties in the N and m estimates from the posterior distribution by either approximation of the covariance matrix or by using standard statistical equations.

A computer code that implements Bayes' rule by combining volumetric and material balance analyses was developed for this research. See Appendices A and B for the main code and modified subroutine, respectively. The main code was developed specifically for Example 1. To adapt the code for other examples requires some modifications to the subroutines to account for differences in fluid PVT properties (Appendix B). This is because the forward model, $g(x)$, depends on the equations governing the fluid PVT properties as a function of pressure.

CHAPTER III

APPLICATION CASES AND RESULTS

Two examples illustrate the use of Bayes' theory to combine volumetric data with the Havlena and Odeh²² material balance equation to estimate N and m and quantify uncertainties. First, I used the data set for a gas-cap drive reservoir with initial volumetric estimates presented by Dake³⁰ in several cases. I introduced uncertainties into the volumetric analysis by assuming standard deviation values to include the ranges of N and m investigated by Dake.³⁰ In other cases, I used different initial estimates to mimic situations where volumetric and material balance results do not coincide. In the second example I used the data set presented by Walsh.¹³ The data set includes average reservoir properties that I used to perform volumetric analysis.

Example 1: Gas-cap Oil Reservoir Reported by Dake³⁰

Problem Statement: A gas-cap drive reservoir was estimated, from volumetric calculations, to have an initial oil volume, N , of 115 MMstb. The ratio of initial gas-cap volume to initial oil volume, m , is uncertain, with a best estimate based on geological information of $m=0.4$. Pertinent PVT, pressure and production data are given in **Table 3.1**. The goal is to determine most likely values of N and m considering both volumetric and material balance data, and to quantify the uncertainties in these estimates. The problem as presented by Dake³⁰ did not specify the uncertainties in the pressure data or the volumetric estimates of N and m , so the results for various combinations of prior probability distributions and observed data errors were investigated.

Case 1: Large Uncertainty in Prior and Small Uncertainty in Pressure Data

This case shows how the posterior and its covariance behave for large uncertainties in the prior ($\sigma_N=35$ MMstb, $\sigma_m=0.13$) and small uncertainty in the pressure data ($\sigma_p=10$ psia). It represents a case in which measured pressures closely represent average

reservoir pressure, because either shut-in times are long or because permeability is high and, thus, pressure stabilization times are short.

Pressure psia	N_p MMstb	R_p scf/stb	B_o rb/stb	R_s scf/stb	B_g rb/scf
3330 (P_i)			1.2511	510	0.00087
3150	3.295	1050	1.2353	477	0.00092
3000	5.903	1060	1.2222	450	0.00096
2850	8.852	1160	1.2122	425	0.00101
2700	11.503	1235	1.2022	401	0.00107
2550	14.513	1265	1.1922	375	0.00113
2400	17.730	1300	1.1822	352	0.00120

*Reprinted from *Fundamentals of Reservoir Engineering*, 8, L.P. Dake, Material Balance Applied to Oil Reservoirs, 91, Copyright (2001), with permission from Elsevier.”

The parameters required to describe the prior distribution (Eq. 2.2) are:

$$\mathbf{x}_{prior} = \begin{bmatrix} N_{prior} \\ m_{prior} \end{bmatrix} = \begin{bmatrix} 115 \\ 0.4 \end{bmatrix} \dots\dots\dots (3.1)$$

$$\mathbf{C}_x = \begin{bmatrix} \sigma_N^2 & \rho\sigma_n\sigma_m \\ \rho\sigma_n\sigma_m & \sigma_m^2 \end{bmatrix} = \begin{bmatrix} 1225 & 4.55\rho \\ 4.55\rho & 0.017 \end{bmatrix} \dots\dots\dots (3.2)$$

The prior distributions shown in **Figs. 3.1 and 3.2**, which are the joint probability distributions calculated by Eq. 2.2, were calculated using 100 uniformly spaced values of N and m . The mode of the distribution corresponds to the prior mean (PM), which is the most probable set of N and m values from volumetric analysis. The difference in the shapes of the distributions in Figs. 3.1 and 3.2 is due to the effect of parameter correlation between N and m . Figs. 3.1 and 3.2 include zero and negative correlation, respectively. Fig. 3.2 has less uncertainty, compared to Fig. 3.1, because it demarcates a smaller region in the space. There is less uncertainty in Fig. 3.2 because correlation

provides more information about the system. This is further illustrated in **Fig. 3.3**, which shows that the uncertainty in the distribution decreases as the magnitude of the correlation coefficient increases. The implication is that parameter correlation is important and should be included in the analysis.

Accordingly, the \mathbf{d}^{obs} required by Eq. 2.3 is:

$$\mathbf{d}^{\text{obs}} = [3150 \ 3000 \ 2850 \ 2700 \ 2550 \ 2400]^T \dots\dots\dots (3.3)$$

The forward model, $g(\mathbf{x})$, defined by Eqs. 2.4-2.7, is used to calculate the likelihood distribution given by Eq. 2.3 (**Fig. 3.4**). Observe in Fig. 3.4 that there are many combinations of N and m with significant probability. This indicates we have significant non-uniqueness when we consider only the material balance solution, even with low error in the pressure data. The likelihood has a clear peak, with maximum likelihood (ML) estimates of $N=145$ MMstb and $m=0.34$.

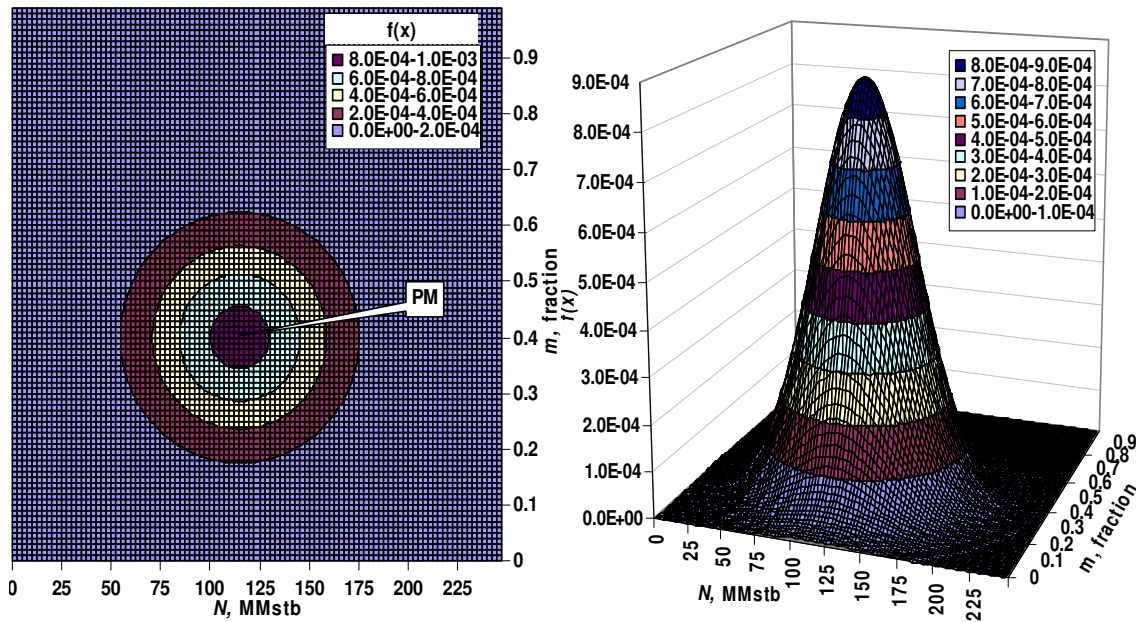


Fig. 3.1—Prior distribution of N and m for case with large uncertainty in the prior for $\rho=0$.

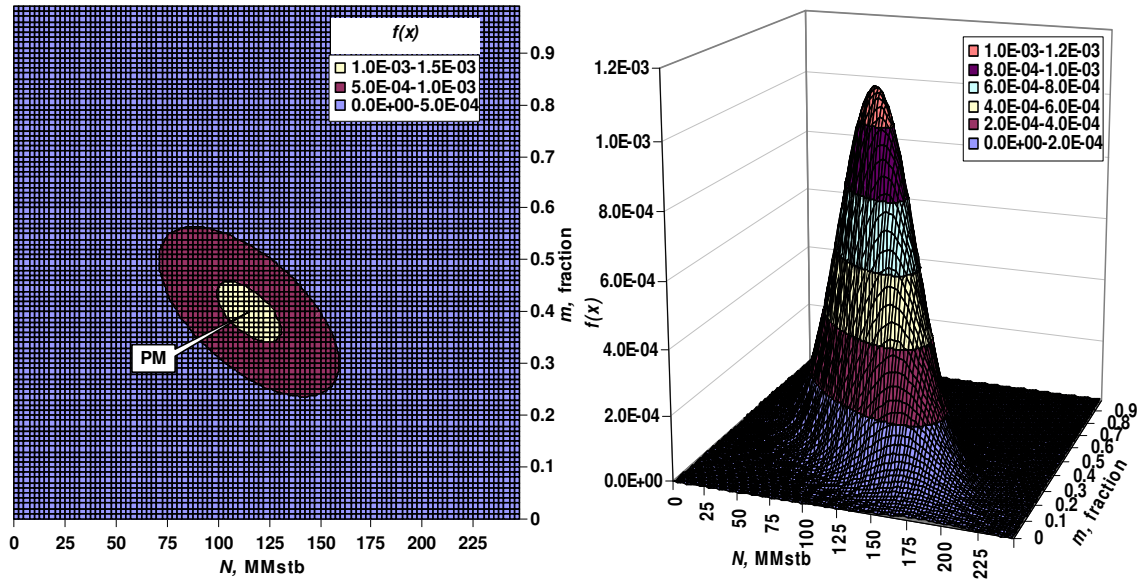


Fig. 3.2—Prior distribution of N and m for case with large uncertainty in the prior for $\rho = -0.6$.

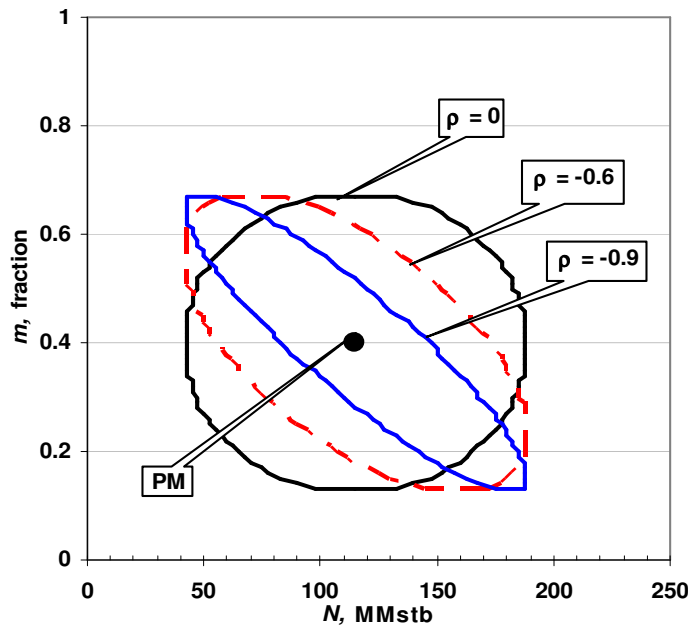


Fig. 3.3—Increasing magnitude of parameter correlation demarcates smaller region in space.

The posterior distribution is the product of the prior and likelihood distributions (Eq. 2.1). We multiply the probabilities from the prior (Fig. 3.1) and likelihood (Fig. 3.4) distributions at every value of $x=N,m$, yielding the posterior distribution (**Fig. 3.5**). Note that the extent of the posterior is considerably smaller than either the prior or likelihood distributions, indicating the reduced uncertainty in the combined volumetric-material balance solution. The MAP solution is $N=127.5$ MMstb and $m=0.42$. The extent of the reduction in the uncertainty is better illustrated in **Fig. 3.6**, in which all three distributions have been plotted on the same graph. The contour lines in Fig. 3.6 represent probability values equal to 10% of the maximum probability from each distribution. Results for this case are summarized in **Table 3.2**. The prior uncertainties in N and m as measured by the standard deviations are each reduced by more than an order of magnitude by integrating the volumetric and material balance analyses.

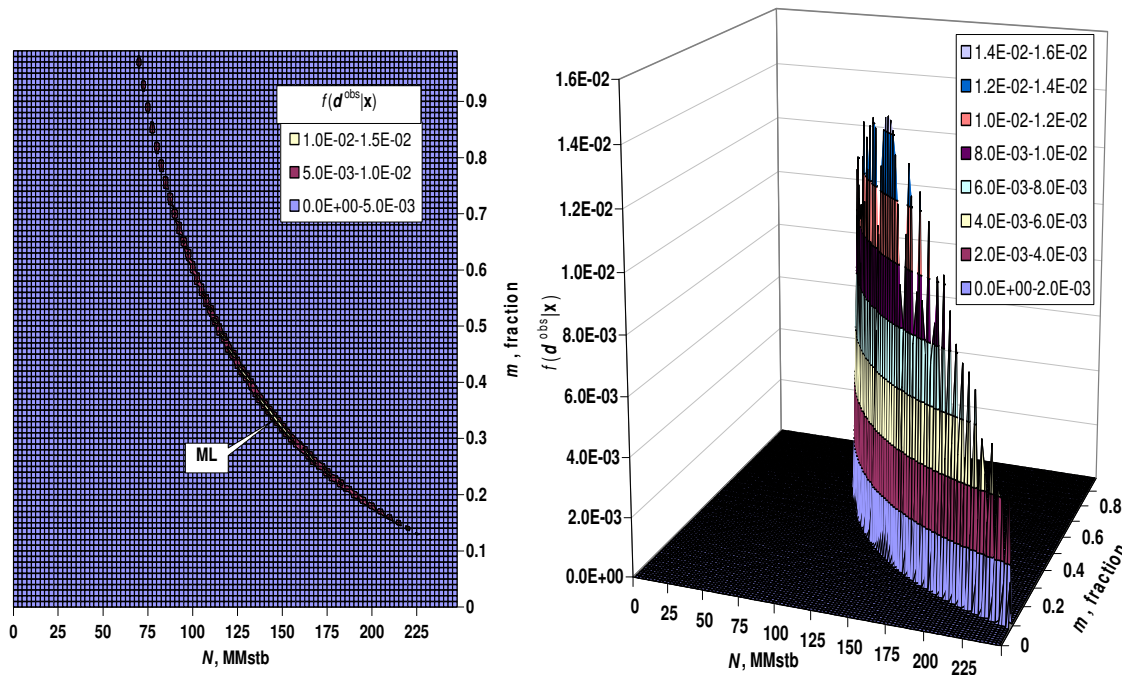


Fig. 3.4—Likelihood distribution of N and m for case with small uncertainty in pressure data.

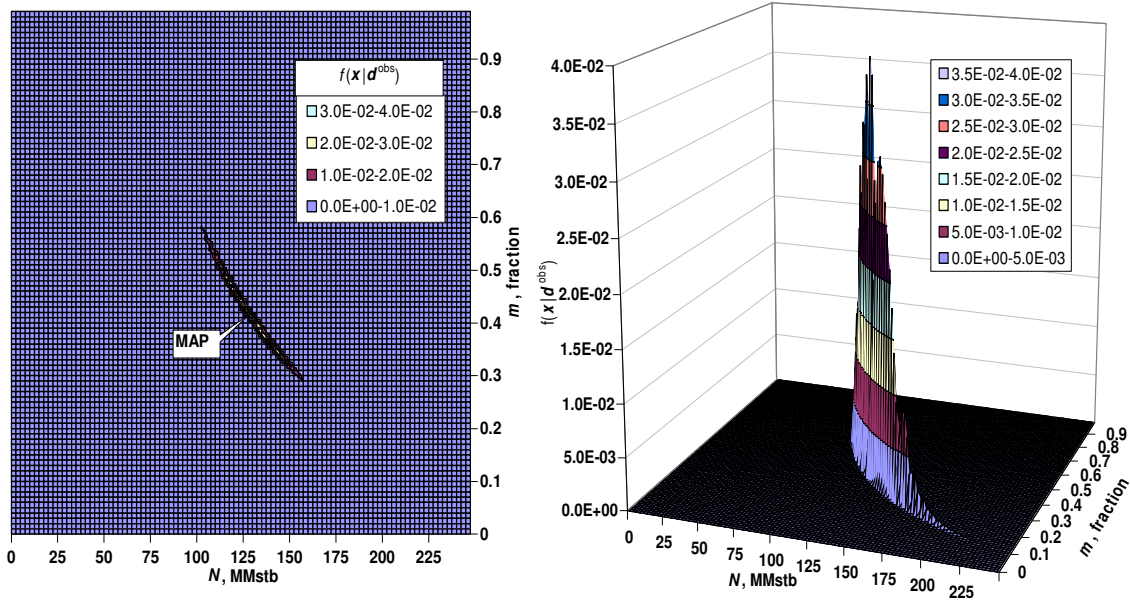


Fig. 3.5—Posterior distribution of N and m for case with small uncertainty in pressure data for $\rho=0$.

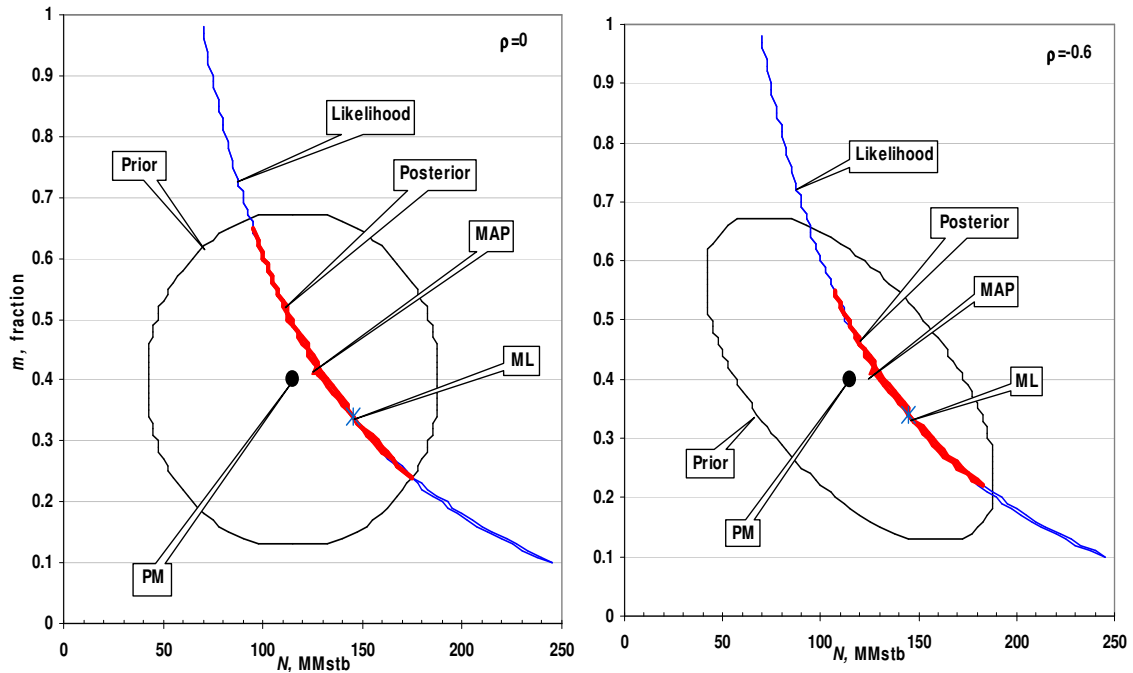


Fig. 3.6—Composite plots show that the posterior distributions lie within the prior and likelihood distributions.

Table 3.2—Summary of Results for Case 1

Table 3.2—Summary of Results for Case 1										
Prior					ML		Posterior			
ρ	N	σ_N	m	σ_m	N	m	N_{MAP}	σ_N	m_{MAP}	σ_m
	MMstb	MMstb			MMstb		MMstb	MMstb		
0	115	35	0.4	0.13	145	0.34	127.5	1.3815	0.42	0.00527
-0.1	115	35	0.4	0.13	145	0.34	127.5	1.3815	0.42	0.00527
-0.2	115	35	0.4	0.13	145	0.34	127.5	1.3814	0.42	0.00527
-0.3	115	35	0.4	0.13	145	0.34	127.5	1.3814	0.42	0.00527
-0.4	115	35	0.4	0.13	145	0.34	127.5	1.3813	0.42	0.00527
-0.5	115	35	0.4	0.13	145	0.34	127.5	1.3812	0.42	0.00527
-0.6	115	35	0.4	0.13	145	0.34	127.5	1.3809	0.42	0.00527
-0.7	115	35	0.4	0.13	145	0.34	127.5	1.3806	0.42	0.00527
-0.8	115	35	0.4	0.13	145	0.34	127.5	1.3798	0.42	0.00527
-0.9	115	35	0.4	0.13	145	0.34	140.0	1.3776	0.36	0.00482

Case 2: Large Uncertainty in Both Prior and Pressure Data

The prior for this case is the same as the previous, except that the uncertainty in pressure data, σ_p , is increased from 10 to 100 psia. As noted by McEwen¹⁰ and Walsh,¹³ uncertainties as high as 100 psia are not unusual, and they can be even much higher in some cases. Some of the uncertainty in pressure data is in the local static pressure measurement, due to gauge error, short shut-in times, or imprecise extrapolation and correction to datum. However, most of the uncertainty is likely in the calculation of average reservoir pressure. Local static pressures may not be representative of average reservoir pressure when there are significant pressure gradients across the reservoir due to low permeability and/or reservoir heterogeneity, and it is often difficult to accurately calculate average reservoir pressure from local static pressures when the data are sparse.

Results for this case are shown in Fig. 3.1, since the prior is the same as in Case 1, and **Figs. 3.7 to 3.10**. The likelihood distribution is shown in Fig. 3.7. The ML is the same as in the previous case, since the ML is the solution to the material balance equation assuming no error in pressures. However, the maximum is not as obvious here, as high probabilities extend over a very long band of N - m combinations. There is much more

non-uniqueness in the material balance solution than in the previous case, due to the increased uncertainty in the pressure data. This is further illustrated in Fig. 3.8, which shows pressure solutions for the three parameter combinations A, B and C indicated on Fig. 3.7. For the purpose of direct comparison, the pressure match for the ML and MAP is plotted on Fig. 3.8 also. All the pressure solutions are in close agreement, and all are well within the $\pm 1\sigma_p$ (± 100 psia) bands shown on Fig. 3.8. Any of these pressure matches would be considered excellent by industry standards.

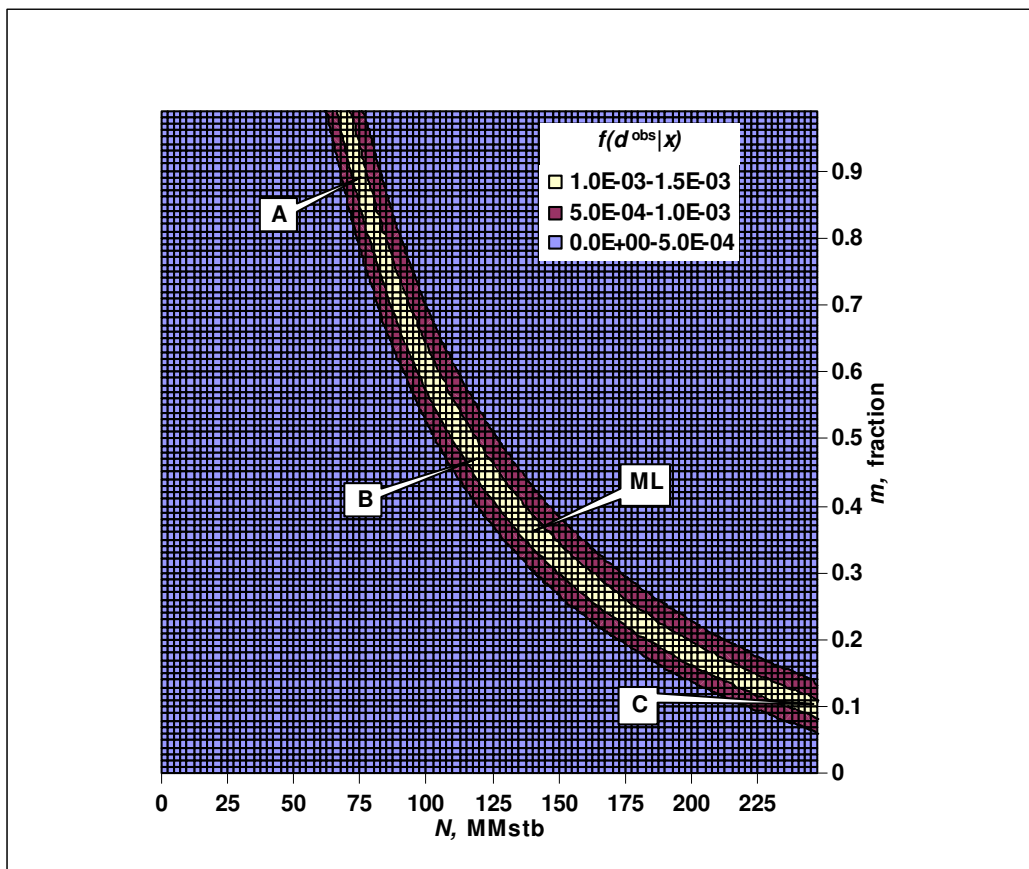


Fig. 3.7—Likelihood distribution for case with large pressure data uncertainty shows considerable non-uniqueness in material balance solution.

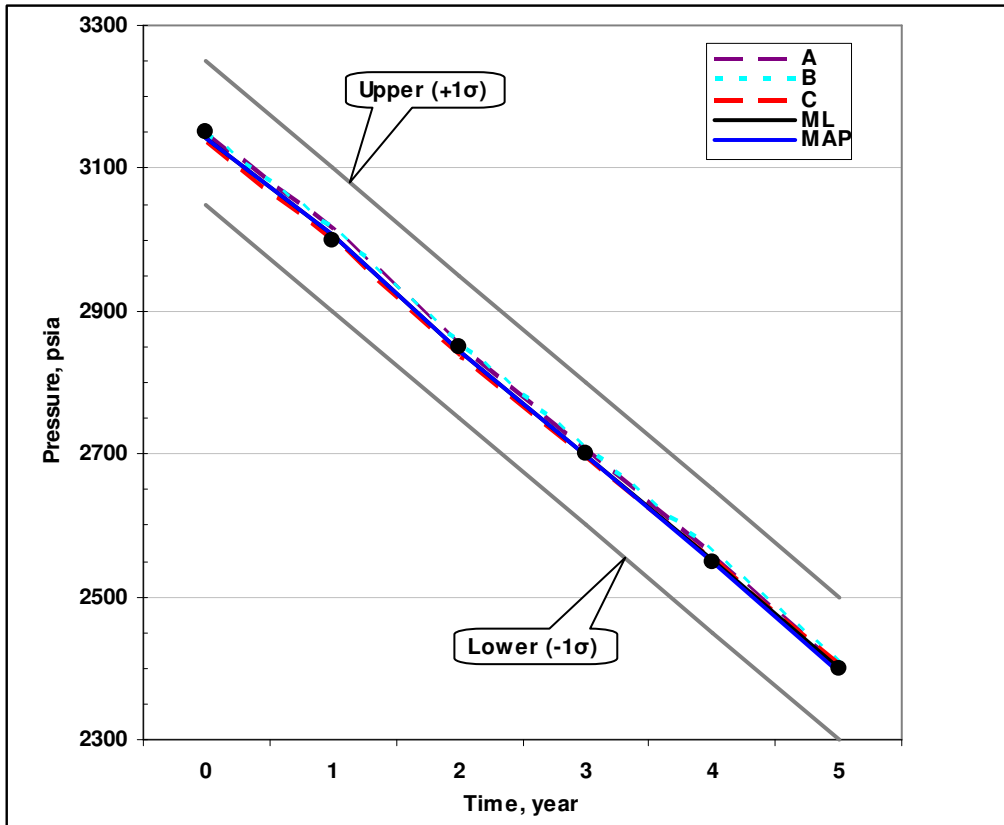


Fig. 3.8—Pressure history match for different N, m solutions (Fig. 4.7) show non-uniqueness of material balance solution.

The posterior distribution is shown in Figs. 3.9 and 3.10. The MAP estimate ($N=127.5$ MMstb and $m=0.41$) is very close to the MAP solution in case 1 ($N=127.5$ MMstb and $m=0.42$). However, there is more uncertainty in this case, as exhibited by the increased width of the posterior distribution (Figs. 3.9 and 3.10) and the larger posterior standard deviations for N and m (Table 3.3). This increased parameter uncertainty is due to the increased uncertainty in the pressure data. Although the uncertainty in the posterior distribution is larger for this case, it is still smaller than the uncertainties in either the prior or likelihood distributions (Fig. 3.10). The material balance data reduce the uncertainty in the prior volumetric estimate, and the volumetric data reduce the non-uniqueness (uncertainty) of the material balance solution.

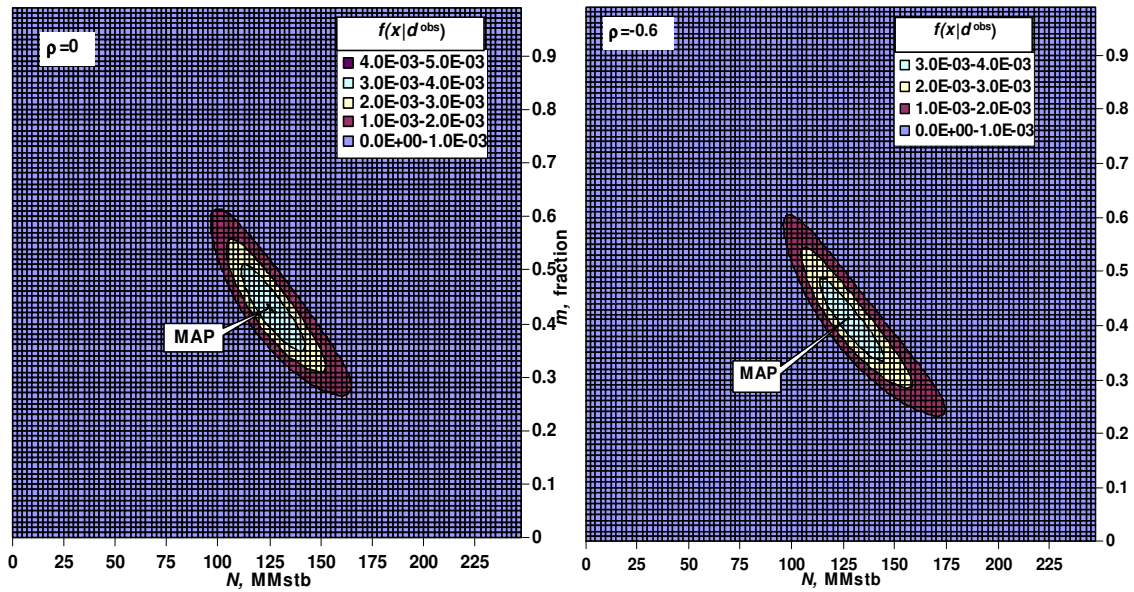


Fig. 3.9—Posterior distributions for cases with large prior and large data uncertainty.

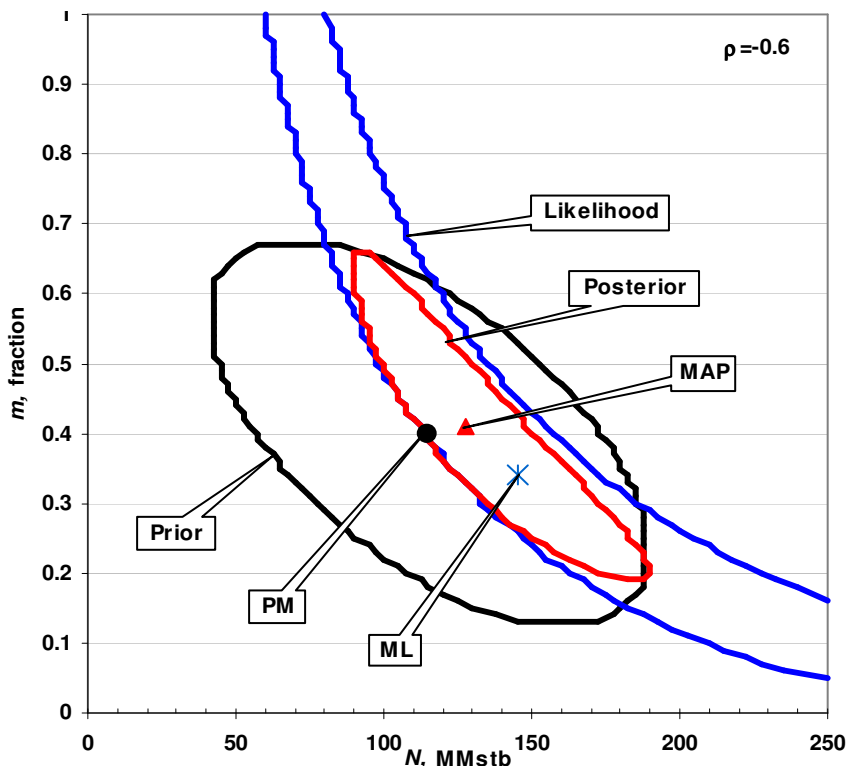


Fig. 3.10—Composite plot for case with large prior and large data uncertainty.

Table 3.3—Summary of Results for Case 2

Table 3.3—Summary of Results for Case 2										
ρ	Prior				ML		Posterior			
	N MMstb	σ_N MMstb	m	σ_m	N MMstb	m	N_{MAP} MMstb	σ_N MMstb	m_{MAP}	σ_m
0	115	35	0.4	0.13	145	0.34	125.0	12.8058	0.43	0.04943
-0.1	115	35	0.4	0.13	145	0.34	125.0	12.8099	0.43	0.04944
-0.2	115	35	0.4	0.13	145	0.34	125.0	12.7990	0.43	0.04939
-0.3	115	35	0.4	0.13	145	0.34	125.0	12.7712	0.43	0.04927
-0.4	115	35	0.4	0.13	145	0.34	125.0	12.7229	0.43	0.04906
-0.5	115	35	0.4	0.13	145	0.34	127.5	12.5381	0.41	0.04717
-0.6	115	35	0.4	0.13	145	0.34	127.5	12.3983	0.41	0.04663
-0.7	115	35	0.4	0.13	145	0.34	127.5	12.2198	0.41	0.04593
-0.8	115	35	0.4	0.13	145	0.34	130.0	11.7451	0.39	0.04321
-0.9	115	35	0.4	0.13	145	0.34	132.5	10.8969	0.37	0.03949

Case 3: Large Uncertainty in Prior With 50 psia Pressure Data Uncertainty

The prior for this case is the same as in Case 2, except that the uncertainty in pressure data, σ_p , is reduced from 100 to 50 psia. The MAP estimate ($N=127.5$ MMstb and $m=0.42$) is very close to the MAP for Case 2. However, there is less uncertainty in this case, as exhibited by the reduced width of the posterior distribution (**Fig. 3.11**), as compared to Fig. 3.10, and the smaller posterior standard deviations for N and m (**Table 3.4**), as compared to Table 3.3.

Cases 1 to 3 confirm that the uncertainty in the posterior estimate of N and m increases as the error in the pressure data is increased. However, for the same error in pressure data, the uncertainty in the posterior estimate is reduced as parameter correlation increases (**Fig. 3.12**). The magnitude of the reduction increases as the correlation between N and m increases. As noted earlier, the increase of the correlation coefficient demarcates a smaller region in the prior distribution, which reduces the uncertainty in the posterior.

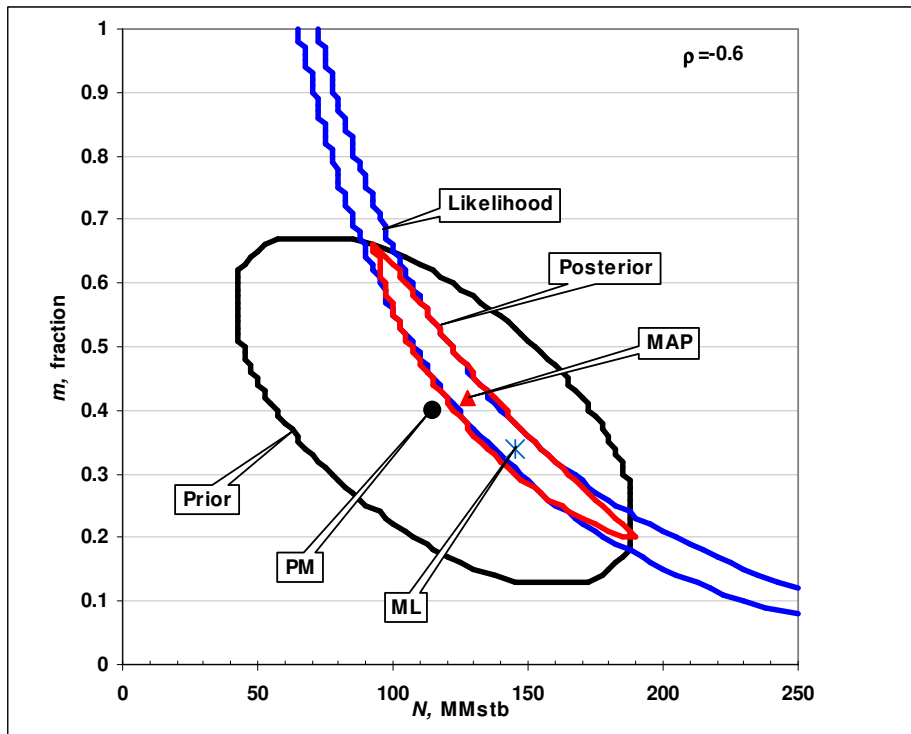


Fig. 3.11—Composite plot for case with large prior and 50 psia pressure data uncertainty.

Table 3.4—Summary of Results for Case 3

ρ	Prior				ML		Posterior			
	N MMstb	σ_N MMstb	m	σ_m	N MMstb	m	N_{MAP} MMstb	σ_N MMstb	m_{MAP}	σ_m
0	115	35	0.4	0.13	145	0.34	127.5	6.7815	0.42	0.02587
-0.1	115	35	0.4	0.13	145	0.34	127.5	6.7814	0.42	0.02587
-0.2	115	35	0.4	0.13	145	0.34	127.5	6.7787	0.42	0.02586
-0.3	115	35	0.4	0.13	145	0.34	127.5	6.7731	0.42	0.02583
-0.4	115	35	0.4	0.13	145	0.34	127.5	6.7637	0.42	0.02579
-0.5	115	35	0.4	0.13	145	0.34	127.5	6.7489	0.42	0.02573
-0.6	115	35	0.4	0.13	145	0.34	127.5	6.7221	0.42	0.02562
-0.7	115	35	0.4	0.13	145	0.34	127.5	6.6851	0.42	0.02548
-0.8	115	35	0.4	0.13	145	0.34	132.5	6.5497	0.39	0.02396
-0.9	115	35	0.4	0.13	145	0.34	135.0	6.3252	0.38	0.02287

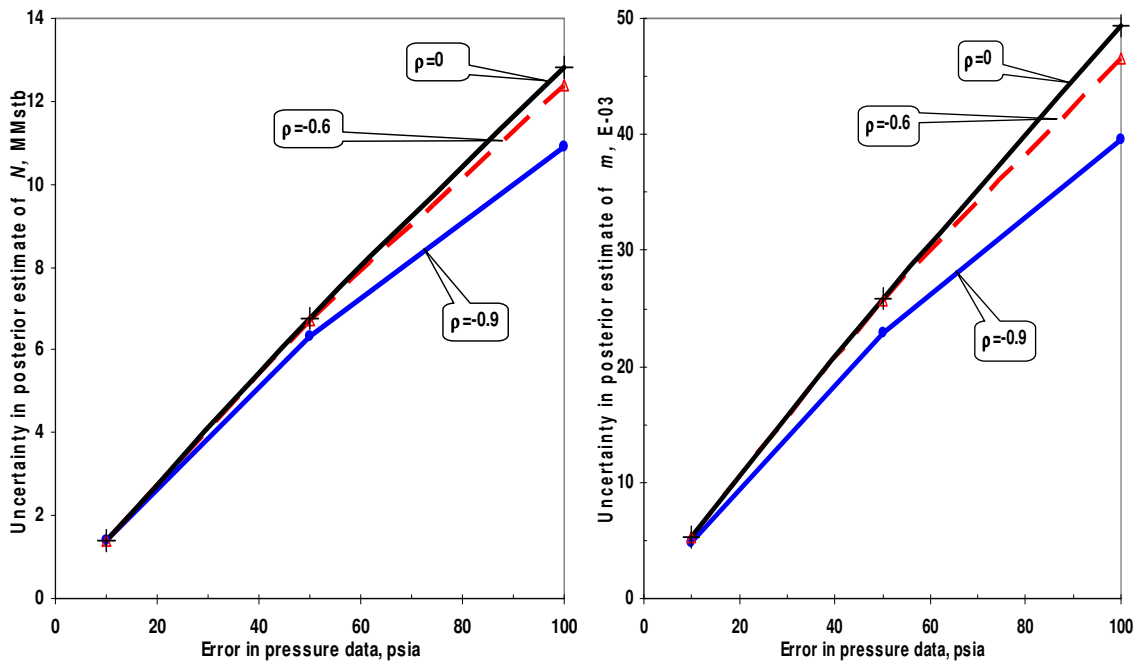


Fig. 3.12—Increasing magnitude of parameter correlation reduces uncertainty in posterior estimates of N and m .

Common features of these first three cases are significant overlap between the prior and likelihood distributions and a ML estimate that lies within the prior solution space. This will be the situation in practice when there is general agreement between estimates from volumetric and material balance analyses. In such situations, the Bayesian results can be meaningful and quite valuable in quantifying the most likely values of N and m and their respective uncertainties. This may not always be the case in practice.

Case 4: Situation With Small Overlap Between Prior and Likelihood

The volumetric estimate (prior mean) for this case was moved so that there is less overlap with the material balance solution (likelihood). The uncertainties in the volumetric estimate and pressure data are the same as in Cases 1 and 2. **Fig. 3.13** is a composite view of the prior, likelihood and posterior distributions. Although the prior mean lies well outside the likelihood distribution and the ML lies well outside the prior distribution, the MAP lies within both the prior and likelihood distributions. With the

Bayesian approach, we are able to reconcile volumetric and material balance analyses that, at first glance, might appear to be quite far apart. If we did not consider the uncertainty in the pressure data (i.e., if we considered only the ML solution), which is common, we might be led to believe that (1) we have a good estimate for N , since the volumetric and material balance solutions for N are in good agreement, and (2) there is a major discrepancy between the volumetric and material balance estimates for m that needs to be resolved. However, when we consider the uncertainties in pressure, we see that the most likely (MAP) value for N is much less than the values from either the volumetric or material balance analyses, and the most likely value for m is greater than both the volumetric and material balance values. With this Bayesian approach, we can reasonably reconcile the differences in the volumetric and material balance analyses even when there is small overlap in the distributions, and we can readily quantify the resulting uncertainties in both N and m .

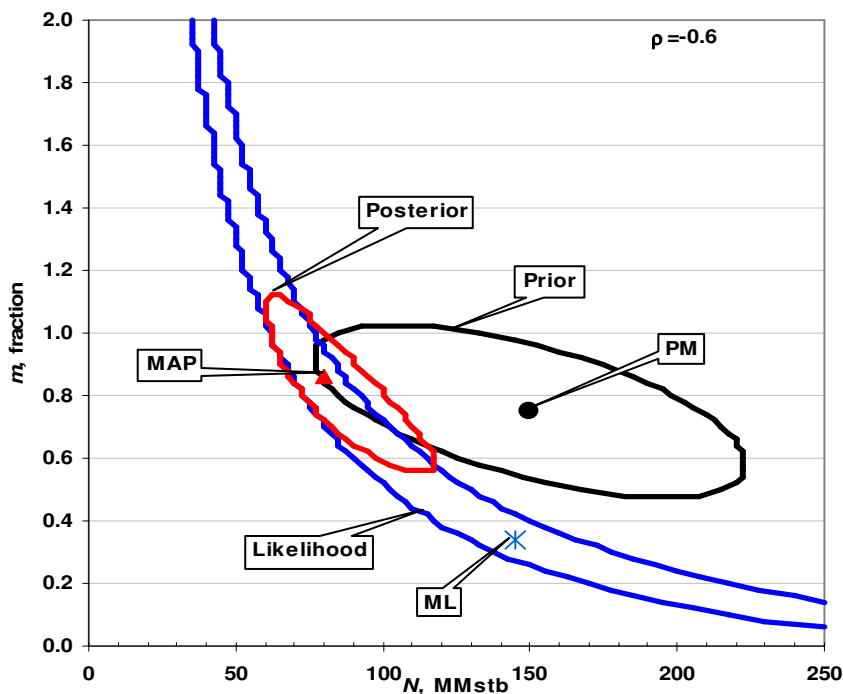


Fig. 3.13—Composite plot for case with small overlap in prior and likelihood shows reconciliation of volumetric and material balance analyses.

Case 5: Situations With Negligible Overlap Between Prior and Likelihood

Volumetric and material balance estimates of OHIP can differ significantly for a variety of reasons. For example, material balance estimates can exceed volumetric estimates when the seismic and well data do not define the full areal extent of the reservoir in the volumetric analysis. Volumetric estimates can exceed material balance estimates when faults or other flow barriers compartmentalize the reservoir, reducing the effective reservoir volume. Three cases in which there is negligible overlap between the prior and likelihood distributions are evaluated.

Case 5a: The volumetric estimate (prior mean) for this case was moved so that there is negligible overlap with the material balance solution (likelihood). The uncertainties in the volumetric estimate and pressure data are the same as in Case 4. **Fig. 3.14** is a composite view of the prior, likelihood and posterior distributions. The MAP is within the likelihood contour, but not within the prior contour. The result is summarized in **Table 3.5**.

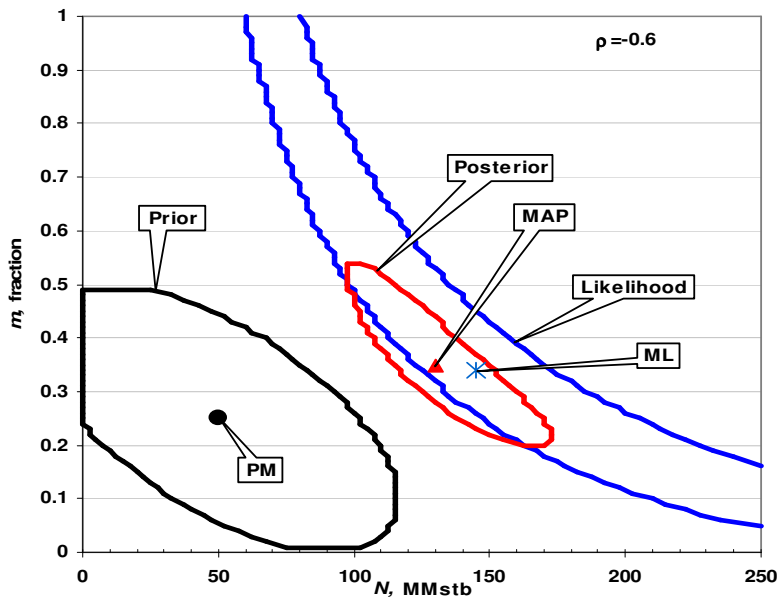


Fig. 3.14— Composite plot for case with large uncertainty in both prior and data, and negligible overlap between prior and likelihood distributions.

Table 3.5—Summary of Results for Case 5a

Table 3.5—Summary of Results for Case 5a										
Prior					ML		Posterior			
ρ	N	σ_N	m	σ_m	N	m	N_{MAP}	σ_N	m_{MAP}	σ_m
	MMstb	MMstb			MMstb		MMstb	MMstb		
0	50	35	0.25	0.13	145	0.34	122.5	12.4839	0.42	0.02587
-0.1	50	35	0.25	0.13	145	0.34	122.5	12.4930	0.42	0.02587
-0.2	50	35	0.25	0.13	145	0.34	125.0	12.3959	0.40	0.02586
-0.3	50	35	0.25	0.13	145	0.34	125.0	12.3713	0.40	0.02583
-0.4	50	35	0.25	0.13	145	0.34	125.0	12.1958	0.39	0.02579
-0.5	50	35	0.25	0.13	145	0.34	127.5	12.0130	0.37	0.02573
-0.6	50	35	0.25	0.13	145	0.34	130.0	11.7584	0.35	0.02562
-0.7	50	35	0.25	0.13	145	0.34	130.0	11.4632	0.34	0.02548
-0.8	50	35	0.25	0.13	145	0.34	132.5	10.8698	0.31	0.02396
-0.9	50	35	0.25	0.13	145	0.34	130.0	9.7244	0.27	0.02287

Case 5b: The likelihood for this case is the same as in Case 5a, except that the uncertainty in the prior has been decreased significantly. With the increased certainty of the volumetric analysis, the MAP moves further from the ML and closer to the PM, and is now outside both the prior and likelihood contours (**Fig. 3.15**). This means that the overlap is at extremely small probability values, i.e., less than 10% of the maximum for the distributions. The uncertainty in the posterior decreases significantly, despite the MAP being far from either volumetric or material balance solutions with significant probability.

Case 5c: The uncertainty in the pressure data is reduced from 100 to 10 psia. With the increased certainty of the pressure data, the MAP is located within the likelihood distribution, although it is far from either the PM or the ML (**Fig. 3.16**). The uncertainty in the posterior is unreasonably low, given that there is negligible overlap between the prior and likelihood distributions.

Figs. 3.15 and 3.16 point out a caveat to using this approach. If we use the method as a black box without looking too closely at the intermediate results and distributions, we

may believe we have an accurate solution given the relatively low uncertainty in the posterior. However, when we look at a composite plot of the distributions, we see that there is clearly something wrong. The prior mean could be in error, but the most likely problem is that we have underestimated the uncertainty in the volumetric analysis or the pressure data (and likely both). Figs. 3.14 and 3.16 have the same prior means and ML's. However, Fig. 3.14 is a more reasonable and believable solution than Fig. 3.16, because of the larger uncertainty in the prior and likelihood distributions. The larger uncertainty in the posterior distribution in Fig. 3.14 is more realistic, given the large uncertainties in the volumetric and material balance estimates. However, it should still give cause for concern, due to the negligible overlap between the prior and likelihood distributions.

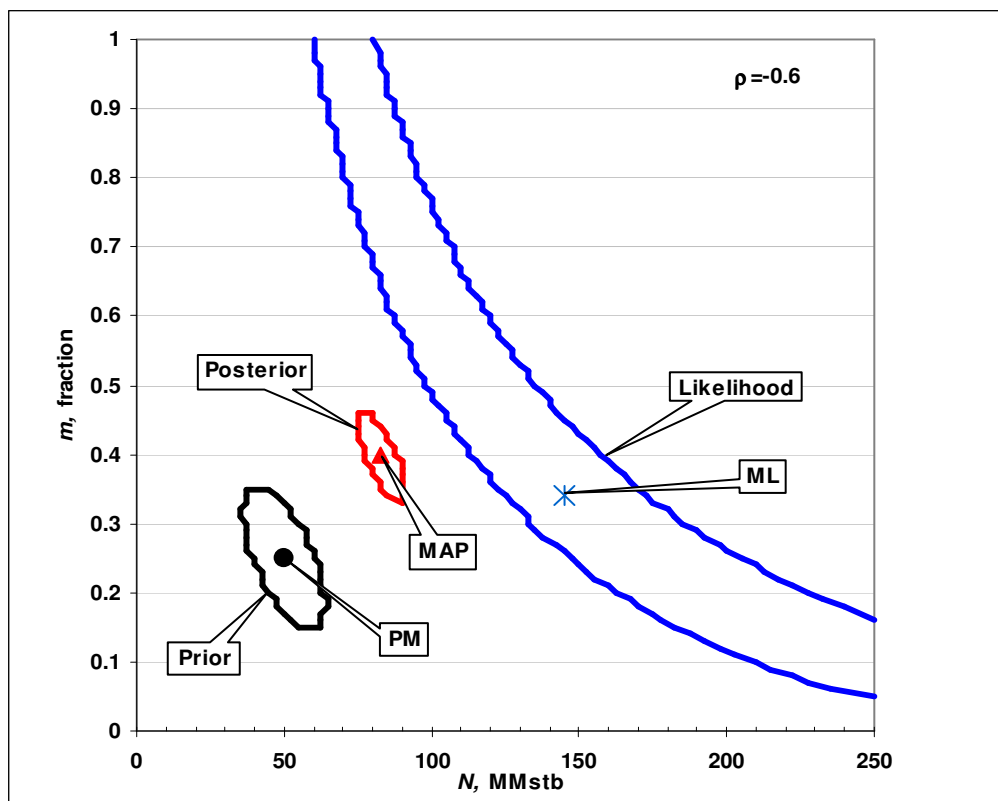


Fig. 3.15—Composite plot for case with small prior uncertainty, large data uncertainty, and negligible overlap between prior and likelihood.

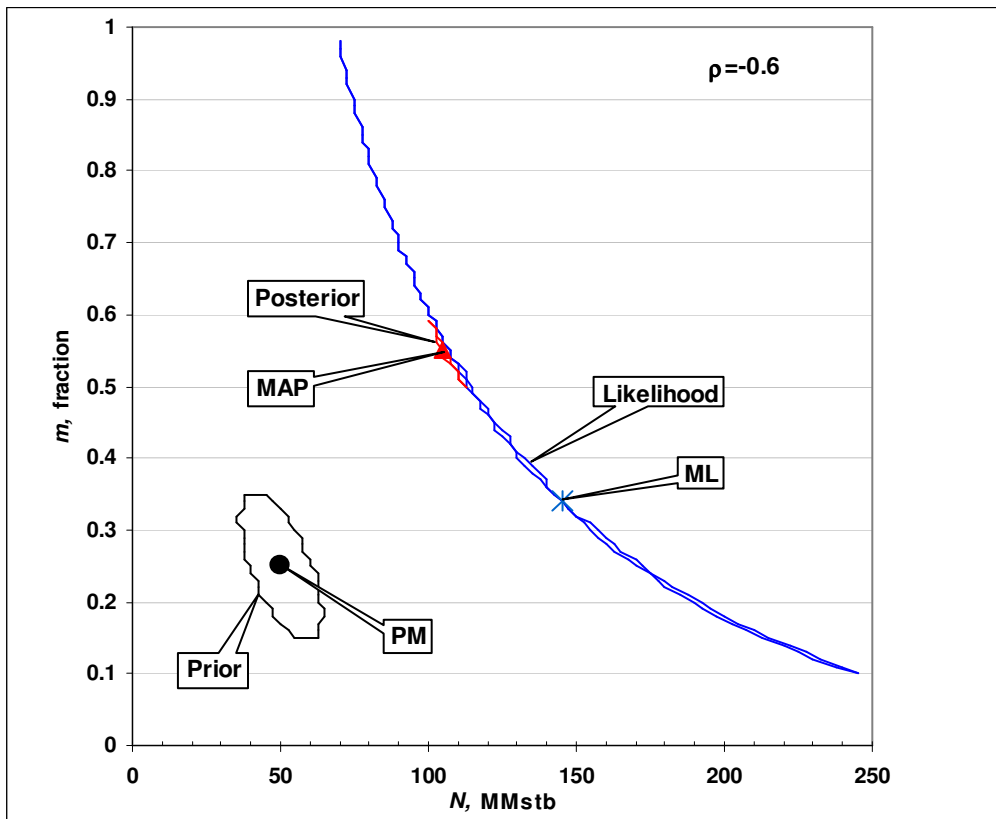


Fig. 3.16—Composite plot for case with small uncertainty in both prior and data, and negligible overlap between prior and likelihood distributions.

While Fig. 3.14 is a better solution, it can be improved further by increasing the uncertainty of the volumetric analysis and/or the pressure data so that the prior and likelihood distributions overlap significantly. As a general guideline, I propose that there should be significant overlap in the prior and likelihood distributions for the posterior distribution to be considered reasonable. When there is negligible overlap between the prior and likelihood distributions, the remedy is to revisit the volumetric and material balance analyses and, in particular, to reevaluate the uncertainties in both. It may further require revising the geological model that formed the basis of the volumetric analysis. This is, of course, very similar to conventional practice: when the OHIP estimates from volumetric and material balance methods do not agree, the geologists and engineers should get together and resolve the differences. The difference is that the proposed

Bayesian approach is a systematic method of formalizing this resolution and quantifying the uncertainties in the combined results.

Implications for Higher-Dimensional Problems

There is significant non-uniqueness in the 2-parameter material balance problem investigated here, particularly when the uncertainty in the observed data is high. Non-uniqueness results in increased uncertainty in the posterior distribution. We will have similar, if not more, non-uniqueness with an increase in the number of parameters, such as in material balance problems with water influx and, particularly, reservoir simulation problems. Thus, if we underestimate the uncertainty in observed data used to calibrate reservoir simulation models, which is common,¹ we will underestimate the uncertainty in reservoir simulation results as well.

One of the advantages of integrating volumetric and material balance analyses using the proposed methodology is that, as demonstrated in the examples above, we can easily sample the entire posterior distribution of OHIP parameters, such as N and m , due to the small number of parameters involved. It is usually impossible to fully sample the posterior distribution of parameters in reservoir simulation models, due to the large number of parameters.

Thus, while we model the reservoir with lower resolution using material balance, we should be able to better quantify the estimates of uncertainty from material balance than from reservoir simulation. Since the primary result from a material balance analysis is a distribution of OHIP, we have to combine this with a distribution of recovery factors to generate a reserves distribution, as done by Salomao and Grell.³¹ The advantage of reservoir simulation, of course, are that we can forecast production and generate a probability distribution of reserves using the simulation model. Perhaps the best use of the volumetric-material balance integration method proposed herein would be in the

calculation of the OHIP distribution prior to reservoir simulation to ensure that the correct OHIP distribution is investigated in the reservoir simulation study.

As with the 2-parameter cases presented here, we should be able to gain insights into the reasonableness of reservoir simulation forecast uncertainties by checking for overlap between the prior and likelihood distributions. This is difficult for multi-parameter reservoir simulation problems because, first, we cannot easily visualize the relationships between the multidimensional probability distributions and, second, it is computationally intensive to do so for a large number of parameters. However, as was demonstrated above, if we do not ensure that there is sufficient overlap between the prior and likelihood distributions, then we will underestimate the uncertainty in reservoir simulation forecasts.

It may be possible to use the pre-posterior,^{25,26} the denominator in Bayes' rule, as a measure of how well the prior and likelihood distribution overlaps. The pre-posterior increases as the degree of the overlap between the prior and likelihood increases (**Fig. 3.17**), as observed in the seven cases discussed above. The suggestion is inconclusive at present and warrants further investigation. More cases need to be evaluated to establish a baseline for perfect overlap.

Example 2: Synthetic Gas-cap Oil Reservoir Presented by Walsh¹³

This is a synthetic gas-cap drive reservoir with reservoir properties, fluid PVT properties and simulated production histories presented in **Tables 3.6 to 3.8**, respectively. Walsh generated three production histories corresponding to $m=0$, 0.25 and 0.5, respectively. I evaluated only one production history, for $m=0.25$.

Walsh¹² did not provide probability distributions for the reservoir parameters and did not provide a prior distribution for N and m . First, I performed the volumetric analysis using Palisade³² @Risk[®] software to generate prior probabilistic estimates of N and m while

assuming various distributions for the input variables (Table 3.6). The means and standard deviations for the normal and lognormal distributions are in parentheses. The three values for the triangular distribution are minimum, most likely and maximum respectively. The reservoir parameters that correlate and the values used for the correlation matrix are in parentheses. Next, BestFit[®] was used to obtain the mean and standard deviation of a normal distribution fitted to the probabilistic estimates of N and m from step one. A correlation coefficient of -0.9 between N and m was calculated using the CORREL function in Excel.[®] The result of the volumetric analysis is summarized in **Table 3.9**. These parameters, mean, standard deviation and correlation coefficient, were used to calculate the prior distribution using Eq. 2.2. Finally, the Bayesian code was used to combine these results with the observed (simulated) production history while considering error in pressure data. The problem as presented by Walsh¹³ did not specify the uncertainties in the pressure data, so I investigated pressure data errors of 10, 50 and 100 psia.

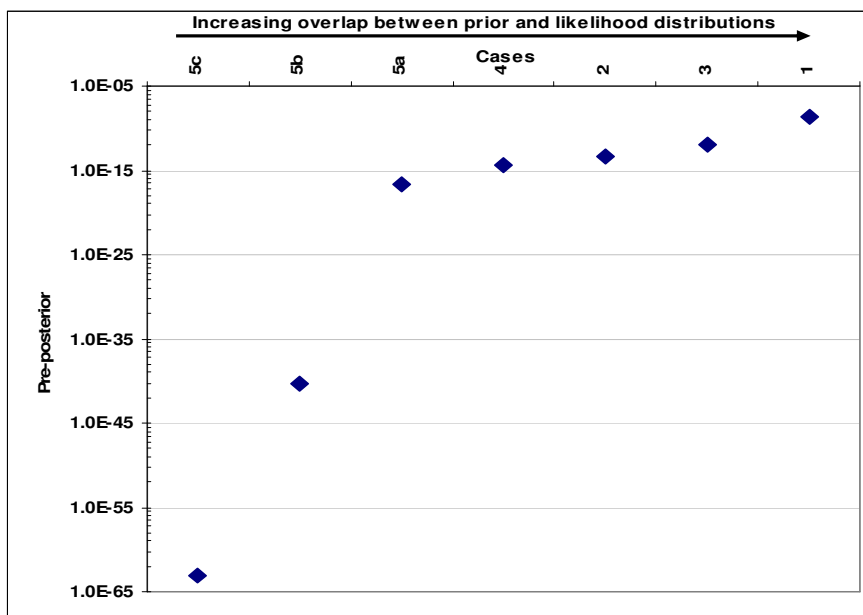


Fig. 3.17—Pre-posterior increases as prior and likelihood overlap significantly.

Table 3.6**—Reservoir Properties for Example 2			
General		Distribution	Correlation matrix
Area, acres	3,796	n/a	n/a
No. of producing wells	48	n/a	n/a
Permeability, md	5	n/a	n/a
Oil-leg thickness, ft	20	Lognormal (20,6.3)	Gas thickness (-1)
Porosity, fraction	0.31	Normal (0.31,0.02)	Water sat. (-0.4)
Initial water sat., fraction	0.20	Lognormal (0.2,0.01)	Porosity (-0.4)
Other	m=0.25		
Gas-cap thickness, ft	5	Triangular (0,5,10)	Oil thickness (-1)
Initial gas-cap gas sat., %PV	80		
OOIP, MMstb	100.0		
OFGIP, Bscf	18.98		
OGIP, Bscf	100.98		

**After Walsh, M.P.: “Effect of Pressure Uncertainty on Material-Balance Plots,” paper SPE 56691 presented at the 1999 SPE Annual Technical Conference and Exhibition, Houston, Texas, 3–6 October, with permission from SPE. Copyright SPE.

Table 3.7†—Black-Oil PVT Properties for Example 2			
Pressure psia	B_o rb/stb	B_g rb/Mscf	R_s scf/stb
1640	1.462	1.926	820.7
1620	1.457	1.951	810.5
1600	1.453	1.977	800.5
1550	1.441	2.047	775.8
1500	1.429	2.126	751.9
1450	1.418	2.211	728.8
1400	1.407	2.305	706.4
1350	1.395	2.406	684.6
1300	1.384	2.514	663.6
1250	1.373	2.630	643.2
1200	1.362	2.753	623.4
1150	1.351	2.884	604.2
1100	1.340	3.023	585.6
1050	1.330	3.169	567.6
1000	1.319	3.323	550.1

†Reprinted from Walsh, M.P.: “Effect of Pressure Uncertainty on Material-Balance Plots,” paper SPE 56691 presented at the 1999 SPE Annual Technical Conference and Exhibition, Houston, Texas, 3–6 October, with permission from SPE. Copyright SPE.

Table 3.8[‡]—Cumulative Oil and Gas Production History for Example 2		
Pressure psia	m=0.25	
	Oil MMstb	Gas Bscf
1640	0.00	0.00
1620	1.36	0.84
1600	2.74	1.69
1550	6.30	3.81
1500	9.67	5.94
1450	12.47	8.08
1400	14.68	10.20
1350	16.44	12.30
1300	17.88	14.37
1250	19.08	16.41
1200	20.10	18.41
1150	20.98	20.36
1100	21.75	22.28
1050	22.42	24.14
1000	23.01	25.96
OOIP	100.0 MMstb	
OFGIP	18.98 Bscf	
OGIP	100.98 Bscf	

[‡]Reprinted from Walsh, M.P.: “Effect of Pressure Uncertainty on Material-Balance Plots,” paper SPE 56691 presented at the 1999 SPE Annual Technical Conference and Exhibition, Houston, Texas, 3–6 October, with permission from SPE. Copyright SPE.

Table 3.9—Summary of Volumetric Analysis	
Parameter	
N , MMstb	92.5
σ_N , MMstb	32.3
m , fraction	0.35
σ_m , fraction	0.26
ρ , decimal	-0.90

Figs. 3.18 to 3.20 illustrate the composite plots for the various ranges of uncertainty in pressure data investigated. There is significant overlap between the prior and the likelihood in all the cases. The reason is because the most-likely values of the parameters used in the volumetric analysis corresponded to the OHIP in the simulation used to generate the production history. Overlap is an important condition for the posterior estimate to be realistic, based on previous results in Example 1. The uncertainty in the prior volumetric estimate is reduced in all the cases after integrating the pressure data using Bayes' theory. The results of the analyses are summarized in **Table 3.10**. There is little difference in posterior uncertainty with a ten-fold difference in pressure error. The reason is because there is considerable uncertainty in the prior and the axes of the prior and likelihood distributions are near parallel.

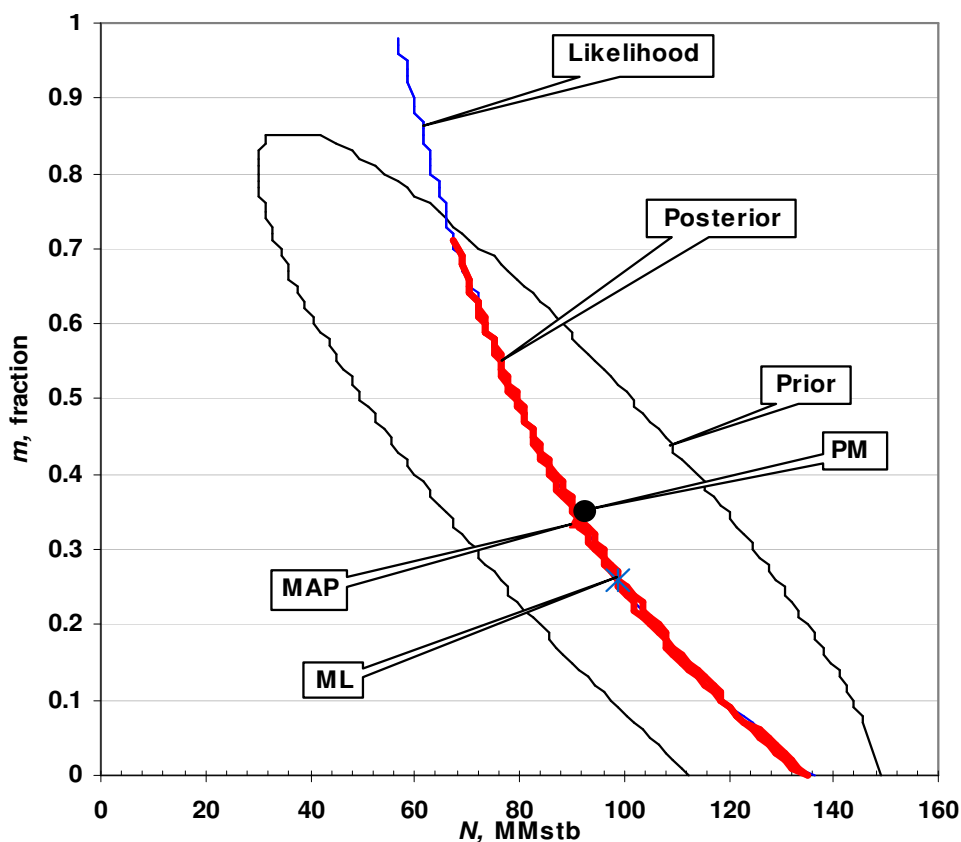


Fig. 3.18—Composite plot for Example 2 with 10 psia error in pressure data.

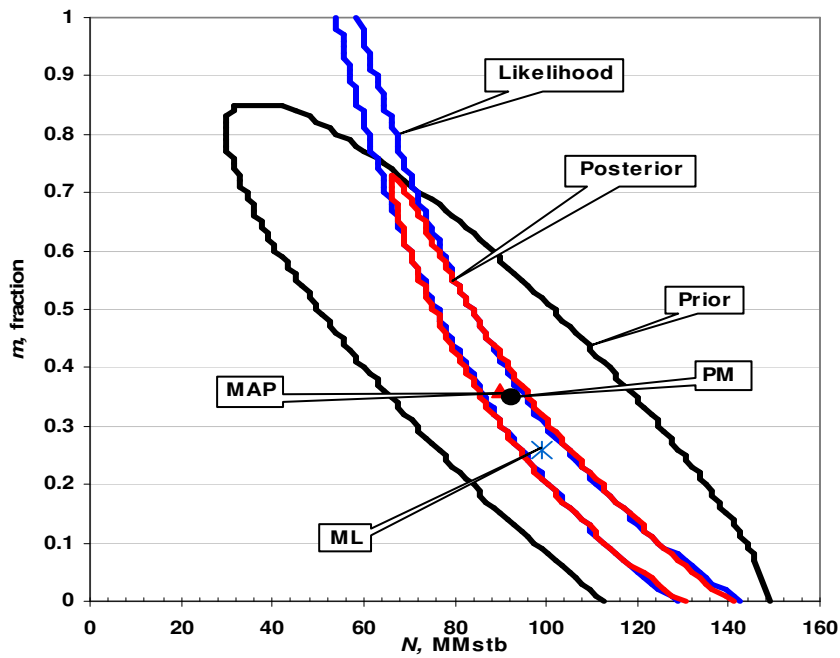


Fig. 3.19—Composite plot for Example 2 with 50 psia error in pressure data.

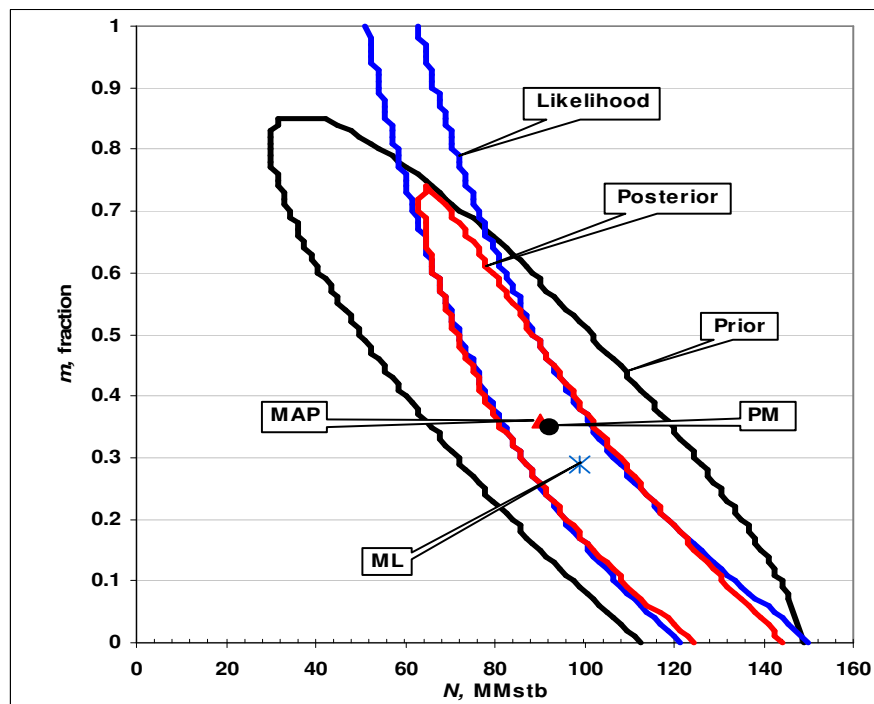


Fig. 3.20—Composite plot for Example 2 with 100 psia error in pressure data.

Table 3.10—Summary of Results for Example 2

Table 3.10—Summary of Results for Example 2										
Prior				Data	ML		Posterior			
N	σ_N	m	σ_m	σ_p	N	m	N_{MAP}	σ_N	m_{MAP}	σ_m
MMstb	MMstb			psia	MMstb		MMstb	MMstb		
92.5	32.3	0.35	0.26	10	99	0.26	91.5	20.1124	0.34	0.23077
92.5	32.3	0.35	0.26	50	99	0.26	90.0	20.0613	0.36	0.23229
92.5	32.3	0.35	0.26	100	99	0.26	90.0	21.6384	0.36	0.23540

CHAPTER IV CONCLUSIONS

The results of this investigation warrant the following conclusions:

1. Bayes' theory can provide a useful framework for combining and reconciling volumetric and material balance analyses and quantifying the uncertainties in the resultant combined estimates of OHIP. An advantage of this approach over reservoir simulation is that, due to the smaller number of parameters, we can readily sample the entire posterior distribution and better quantify the uncertainty in OHIP.
2. Solutions to material balance problems may be highly non-unique (uncertain), even for 2-parameter problems such as in gas-cap drive oil reservoirs. Non-uniqueness increases significantly with increasing error in the observed pressure data.
3. The uncertainty in the posterior estimates reduces as the magnitude of the parameter correlation increases for the cases investigated in this thesis.
4. Use of the Bayesian approach yields combined OHIP parameter estimates with lower uncertainties than from either volumetric or material balance estimates. The material balance data reduce the uncertainties in the prior volumetric estimate, and the volumetric data reduce the non-uniqueness (uncertainties) of the material balance solution.
5. If the prior (volumetric) and likelihood (material balance) probability distributions do not overlap significantly, the approach may result in unrealistically low uncertainties in the posterior (combined) OHIP parameter estimates. When there is insufficient overlap, the volumetric and material balance analyses should be revisited and the uncertainties of each reevaluated.

NOMENCLATURE

B_g	=	gas formation volume factor, rb/scf
B_{gi}	=	initial gas formation volume factor, rb/scf
B_o	=	oil formation volume factor, rb/stb
B_{oi}	=	initial oil formation volume factor, rb/stb
$\det()$	=	determinant
E_g	=	gas expansion factor, rb/stb
E_o	=	oil expansion factor, rb/stb
F	=	underground withdrawal of fluid, rb
m	=	ratio of gas-cap volume to oil volume, fraction
N	=	original oil in place, stb
n_d	=	number of observed data
n_x	=	number of model parameter
N_p	=	cumulative oil recovery, stb
R_p	=	cumulative gas oil ratio, scf/stb
R_s	=	solution gas oil ratio, scf/stb
R_{si}	=	initial solution gas oil ratio, scf/stb
ρ	=	correlation coefficient
σ	=	standard deviation
π	=	3.1416

Subscripts

D	=	data
x	=	model

Superscripts

obs	=	observed
T	=	transpose

REFERENCES

1. Capen, E.C.: "The Difficulty of Assessing Uncertainty," *JPT* (August 1976) 843.
2. Smith, P.J. and Buckee, J.W.: "Calculating In-Place and Recoverable Hydrocarbons: A Comparison of Alternative Methods," paper SPE 13776 presented at the 1985 SPE Hydrocarbon Economics and Evaluation Symposium, Dallas, Texas, 14–15 March.
3. Capen, E.C.: "A Consistent Probabilistic Definition of Reserves," *SPE* (February 1996) 23.
4. McVean, J.R.: "The Significance of Risk Definition on Portfolio Selection," paper SPE 62966 presented at the 2000 SPE Annual Technical Conference and Exhibition, Dallas, Texas, 1–4 October.
5. Cronquist, C.: *Estimation and Classification of Reserves of Crude Oil, Natural Gas, and Condensate*, SPE, Richardson, Texas (2001).
6. Calson, M.R.: "Tips, Tricks and Traps of Material Balance Calculations," *J. Cdn. Pet. Tech.* (December 1997) 34.
7. Dorr, S., Testerman, J. and Bercegeay P.: "Estimation of Reservoir Oil-In-Place Using Statistical Confidence Intervals," paper SPE 4297 available from SPE, Richardson, Texas (1972).
8. White, D.A. and Gehman, H.M.: "Methods of Estimating Oil and Gas Resources," *AAPG Bull.* (December 1979) **63**, 2183.
9. Mian, M.A.: *Project Economics and Decision Analysis. Vol. II: Probabilistic Models*, PennWell Corp., Tulsa, Oklahoma (2002).
10. McEwen, C.R.: "Material Balance Calculations With Water Influx in the Presence of Uncertainty in Pressures," *Trans., AIME* (1962) **225**, 120.
11. Fair, W.B.: "A Statistical Approach to Material Balance Methods," paper SPE 28629 presented at the 1994 SPE Annual Technical Conference and Exhibition, New Orleans, Louisiana, 25–28 September.
12. Wang, B. and Hwan, R.R.: "Influence of Reservoir Drive Mechanism on Uncertainties of Material Balance Calculations," paper SPE 38918 presented at the

- 1997 SPE Annual Technical Conference and Exhibition, San Antonio, Texas, 5–8 October.
13. Walsh, M.P.: “Effect of Pressure Uncertainty on Material-Balance Plots,” paper SPE 56691 presented at the 1999 SPE Annual Technical Conference and Exhibition, Houston, Texas, 3–6 October.
 14. Dake, L.P.: *The Practice of Reservoir Engineering*, rev. ed., Elsevier, Amsterdam (2001).
 15. Pletcher, J.L.: “Improvements to Reservoir Material-Balance Methods,” *SPEREE* (February 2002) 49.
 16. Stoltz, L.R., Jones, M.S. and Wadsley, A.W.: “Probabilistic Reserves Assessment Using a Filtered Monte Carlo Method in a Fractured Limestone Reservoir” paper SPE 39714 presented at the 1998 SPE Asia Pacific Conference on Integrated Modeling for Asset Management, Kuala Lumpur, Malaysia, 23–24 March.
 17. Floris, F.J.T., Bush, M.D., Cuypers, M., Roggero, F. and Syversveen, A-R.: “Methods for Quantifying the Uncertainty of Production Forecasts: A Comparative Study,” *Petroleum Geoscience* (2001) **7**, S87.
 18. Glimm, J., Hou, S., Lee, Y., Sharp, D. and Ye K.: “Prediction of Oil Production with Confidence Intervals,” paper SPE 66350 presented at the 2001 SPE Reservoir Simulation Symposium, Houston, Texas, 11–14 February.
 19. Vega, L., Rojas, D. and Datta-Guptta, A.: “Scalability of the Deterministic and Bayesian Approaches to Production Data Integration into Field-Scale Reservoir Models,” paper SPE 79666 presented at the 2003 SPE Reservoir Simulation Symposium, Houston, Texas, 3–5 February.
 20. Lepine, O.J., Bissell, R.C., Aanonsen, S.I., Pallister, I.C. and Baker, J.W.: “Uncertainty Analysis in Predictive Reservoir Simulation Using Gradient Information,” *SPEJ* (September 1999) 251.
 21. Hwan, R.R.: “Improved Material Balance Calculations by Coupling with a Statistics-Based History-Matching Program,” paper SPE 26244 presented at the 1993 SPE Petroleum Computer Conference, New Orleans, Louisiana, 11–14 July.

22. Havlena, D. and Odeh, A.S.: "The Material Balance as an Equation of a Straight Line," *Trans.*, AIME (1963) **231**, 896.
23. Tarantola, A.: *Inverse Problem Theory-Methods for Data Fitting and Model Parameter Estimation*, Elsevier, New York (1987).
24. Scales, J.A., Smith, M.L., and Treitel, S.: *Introductory Geophysical Inverse Theory*, Samizdat Press, Golden, Colorado (1997).
25. Clemen, R.T. and Reilly, T.: *Making Hard Decisions with DecisionTools*, 2nd rev. ed., Duxbury, Pacific Grove, California (2001).
26. Winkler, R.L.: *An Introduction to Bayesian Inference and Decision*, Holt, Rinehart and Winston, Inc., New York (1972).
27. Murtha, J.: "Risk Analysis for the Oil Industry," Supplement to *Hart's E&P*, (August 2001) 2.
28. Duijndam, A.J.W.: "Bayesian Estimation in Seismic Inversion. Part I: Principles," *Geophysical Prospecting* (1988) **36**, 878.
29. Montgomery, D.C., and Runger, G.C.: *Applied Statistics and Probability for Engineers*, 3rd ed., John Wiley & Sons Inc., New York (2003).
30. Dake, L.P.: *Fundamentals of Reservoir Engineering*, Elsevier, Amsterdam (2001).
31. Salomao, M.C., and Grell, A.P.: "Uncertainty in Production Profiles on the Basis of Geostatistic Characterization and Flow Simulation," paper SPE 69477 presented at the 2001 SPE Latin American and Caribbean Petroleum Engineering Conference, Buenos Aires, Argentina, 25–28 March.
32. Palisade @Risk, and BestFit, vers. 4.5.4, Palisade Corporation, Ithaca, New York (2004).

APPENDIX A
BAYESIAN MAIN CODE

```

c  Program to integrate volumetric and material balance analyses.
  implicit double precision(a-h,o-z)
  PARAMETER(nrand=100,ndata=6,nparam=2)
  Dimension aN(nrand),am(nrand),d(ndata),aNp(ndata),Rp(ndata),
  *pprior(nrand,nrand),pdata(nrand,nrand),ppost(nrand,nrand),
  *Gsen(ndata,nparam),Cd(ndata,ndata),Cm(nparam,nparam),g(ndata),
  *Gt(nparam,ndata),CdGs(ndata,nparam),GtCdGs(nparam,nparam),
  *Cmapinv(nparam,nparam),Cmap(nparam,nparam),objinv(nrand,nrand),
  *Cprmx(nparam,nparam),Cprmxinv(nparam,nparam),Prm(nrand,nparam),
  *PrmT(nparam,nrand),CpPT(nparam,nrand),PCmPT(nrand,nrand)

  open(3,file = 'preliminp1.dat')
  open(2,file = 'prelimout.out')
  open(6,file = 'check.out')
  open(8,file = 'MAP_Estimate.dat')
  open(9,file = 'sensivity.out')
  open(11,file='Cmapinv.dat')
  open(13,file='gcal_MAP.dat')
  open(15,file='mean-covariance_imethod_1.dat')
  open(16,file='Cmap_imethod_0.dat')
  open(17,file='Cmap_imethod_2.dat')
  open(18,file='negative_pressure.dat')
  open(21,file='Cprmx.dat')
  open(23,file='Cprmxinv_chile.dat')
  open(26,file='PrmT_chile.dat')

  read(3,*)n,m,nd,aNavg,amavg,sdN,sdm,cor,sdd,Boi,Bgi,Rsi
c  Reading the i_method
c  i_method = 0—Use approximated analytical method with the exact Covariance Matrix
c  i_method = 1—Use numerical method
c  i_method = 2—Use approximated analytical method with the covariance of the prior
c                calculated from the numerical method
      read(3,*)i_method
      do 10 i=1,nd
10    read(3,*)d(i),aNp(i),Rp(i)
      do 20 i=1,n
20    read(3,*)aN(i),am(i)

c  Calculating the  $1/((2 * \pi)^{(m/2))*((\det(Cm))^{(0.5)})$  &

```

```

c          1/(((2 * pi)^(nd/2))*((det(Cd))^(0.5)))
c          for 2x2 matrix of Cm and diagonal matrix of Cd
c*****Start Calculation*****
      corS=cor**2.
      sdNS=sdN**2.
      sdmS=sdm**2.
      sddS=sdd**2.
      cstpr=1./(((44./7.)**(m/2.))*(sdNS*sdmS-(corS*sdNS*sdmS))**0.5)
      cstexp=0.5/(1-corS)
      cstdat=1./(((44./7.)**(nd/2.))*(sdd**nd))
c***** form the matrix Cprmx *****
      do i=1,m
        do j=1,m
          Cprmx(i,j)=0.0
          If(i.eq.j)then
            if (i.eq.1) then
              Cprmx(i,j)=sdNS
            else
              Cprmx(i,j)=sdmS
            endif
          endif
          if(i.eq.1) then
            if(j.eq.2) then
              Cprmx(i,j)=cor*sdN*sdm
            endif
          endif
          if(i.eq.2) then
            if(j.eq.1) then
              Cprmx(i,j)=cor*sdN*sdm
            endif
          endif
        enddo
      enddo
c***** write the matrix Cprmx *****
      do i=1,m
        write(21,*)(Cprmx(i,j),j=1,m)
      enddo
      Close(21)
c***** call the subroutine prmxinversion to get the invese of the matrix Cprmxinv ****
      CALL prmxinversion
c***** saving the inverse of the matrix Cprmxinv *****
      open(22,file='Cprmxinv.dat')
      do i=1,m
        read(22,*)(Cprmxinv(i,j), j=1,m)

```



```

        enddo
c***** writing the inverse of the matrix Cprmxinv *****
    do i=1,m
        write(23,*)(Cprmxinv(i,j), j=1,m)
    enddo
c***** call the subroutine prpdf to set up the prior pdf *****
    do j=1,n
        CALL prpdf(n,m,j,aNavg,amavg,aN(j),am(j),Prm(j,1),Prm(j,2))
    enddo
        do j=1,n
            write(25,*)(Prm(j,i), i=1,m)
        enddo
c***** form matrix Prm^T in array PrmT *****
    do i=1,m
        do j=1,n
            PrmT(i,j)=Prm(j,i)
        enddo
    enddo
        do i=1,m
            write(26,99)(PrmT(i,j), j=1,n)
99    format(100(F8.2))
    enddo
c*****PDF for the prior-Likelihood-Posterior*****
c    iflag=0
c    Save the maximum of the liklihood and the posterior in array amaxl, amax
    amaxl=0.0
    amax=0.0
    aobjinvmax=0.0
    do 30 i=1,n
    do 31 k=1,n
        pprior(i,k)=cstpr*r*dexp(-cstexp*(((aN(k)-aNavg)**2.)/sdNS)-
&(2.*cor*(aN(k)-aNavg)*(am(i)-amavg)/(sdN*sdm))+
&(((am(i)-amavg)**2.)/sdmS)))
        sum=0.0
        sum1=0.0
        j=0
35    j=j+1
c***** calling subroutine iterate to use Newton method to get g(m) *****
        Call iterate(i,k,j,aN(k),am(i),aNp(j),Rp(j),Boi,Bgi,Rsi,g(j),
& dfpdp)
        write(6,*)g(j)
        IF(g(j).lt.0.0.or.g(j).gt.3330.0)THEN
            pdata(i,k)=0.0
            ppost(i,k)=0.0

```

```

        objinv(i,k)=0.0
        write(18,*)aN(k),am(i)
Else
  if(j.ne.nd)then
    sum1=sum1+(1./(((d(j)-g(j))**2.)*(1./sddS)))
    sum=sum+(((d(j)-g(j))**2.)*(1./sddS))
    goto 35
  else
    sum1=sum1+(1./(((d(j)-g(j))**2.)*(1./sddS)))
    sum=sum+(((d(j)-g(j))**2.)*(1./sddS))
    endif
    pdata(i,k)=cstdat*dexp(-0.5*sum)
    objinv(i,k)=sum1
    ppost(i,k)=pprior(i,k)*pdata(i,k)
  if(pdata(i,k).Gt.amax1)then
    amax1=pdata(i,k)
    aNmax1=aN(k)
    ammax1=am(i)
    kmax1=k
    imax1=i
  endif
  if(pdata(i,k).lt.1E-20)then
    pdata(i,k)=0.0
  endif
  if(objinv(i,k).Gt.aobjinvmax)then
    aobjinvmax=objinv(i,k)
    aNobjinv=aN(k)
    amobjinv=am(i)
    kobjinv=k
    iobjinv=i
  endif
  if(ppost(i,k).Gt.amax)then
    amax=ppost(i,k)
    aNmax=aN(k)
    ammax=am(i)
    kmax=k
    imax=i
  endif
  if(ppost(i,k).lt.1E-20)then
    ppost(i,k)=0.0
  endif
ENDIF
31  continue
30  continue

```

```

c*****Writing the PDF distribution*****
      write(2,*)"the prior"
      do 50 i=1,n
        write(2,4)(pprior(i,k), k=1,n)
4    format(100(F20.4))
50   continue
      write(2,*)"the data error"
      do 60 i=1,n
        write(2,5)(pdata(i,k), k=1,n)
5    format(100(E20.4E3))
60   continue
      write(2,*)"the posterior"
      do 70 i=1,n
        write(2,6)(ppost(i,k), k=1,n)
6    format(100(E20.4E3))
70   continue
      If(i_method.eq.0)then
c***** getting sensivity Matrix at the MAP *****
          do j=1,nd
c***** calling subroutine iterate to use Newton method to get g(m) at MAP *****
            Call iterate(imax,kmax,j,aNmax,ammax,aNp(j),Rp(j),Boi,Bgi,Rsi,
            & g(j),dfpdpmax)
            write(13,*)j,g(j),dfpdpmax
            Call Sensivity(m,nd,j,g(j),dfpdpmax,aNmax,ammax,Boi,Bgi,Rsi,
            & Gsen(j,1),Gsen(j,2))
            enddo
c***** writing sensitivity *****
          do j=1,nd
            write(9,*)(Gsen(j,k), k=1,m)
          enddo
c***** form the matrix Cd^-1 in array Cd *****
          do i=1,nd
            do j=1,nd
              cd(i,j)=0.0
              If(i.eq.j)then
                cd(i,j)=1./sddS
              endif
            enddo
          enddo
c***** form matrix G^T at the MAP in array GsT *****
          do i=1,m
            do j=1,nd
              Gt(i,j)=Gsen(j,i)
            enddo
          enddo

```

```

        enddo
c***** form the matrix (Cd^-1 * G) in array CdGs *****
    do i=1,nd
        do j=1,m
            sum1=0.0
            do k=1,nd
                sum1=sum1+(cd(i,k)*Gsen(k,j))
            enddo
            CdGs(i,j)=sum1
        enddo
    enddo
c***** form the matrix G^T * CdGs in array GtCdGs *****
    do i=1,m
        do j=1,m
            sum2=0.0
            do k=1,nd
                sum2=sum2+(Gt(i,k)*CdGs(k,j))
            enddo
            GtCdGs(i,j)=sum2
        enddo
    enddo
c***** form the matrix G^T * Cd^-1 * G + Cm^-1 in array Cmapinv *****
    do i=1,m
        do j=1,m
            Cmapinv(i,j)=GtCdGs(i,j)+Cprmxinv(i,j)
        enddo
    enddo
c***** write the matrix Cmapinv which is the Hessian *****
    do i=1,m
        write(11,*)(Cmapinv(i,j),j=1,m)
    enddo
    Close(11)
c**** call the subroutine matrixinversion to get the invese of the matrix Cmapinv ****
    CALL matrixinversion
c***** saving the inverse of the matrix Cmapinv in array Cmap *****
    open(12,file='Cmap.dat')
    do i=1,m
        read(12,*)(cmap(i,j), j=1,m)
    enddo
c***** writing the inverse of the matrix Cmapinv *****
    do i=1,m
        write(16,*)(cmap(i,j), j=1,m)
    enddo
    sdNpst=cmap(1,1)**0.5

```

```

    sdpst=cmap(2,2)**0.5
    corpst=cmap(1,2)/(sdNpst*sdpst)
c***** writing the Maximum likelihood and the Maximum A posteriori estimate *****
    write(8,*)amax1,aNmax1,amax1,imax1,kmax1
    write(8,*)amax,aNmax,amax,imax,kmax,sdNpst,sdpst,corpst
    ELSEIF(i_method.eq.1)then
c***** calculating Mean and Covariance of the Prior using the numerical form*****
    sum3=0.0
    do i=1,n
        do k=1,n
            sum3=sum3+(pprior(i,k))
        enddo
    enddo
    sum4=0.0
    do i=1,n
        do k=1,n
            sum4=sum4+(aN(k)*pprior(i,k))
        enddo
    enddo
    sum4=sum4/sum3
    sum5=0.0
    do i=1,n
        do k=1,n
            sum5=sum5+(am(i)*pprior(i,k))
        enddo
    enddo
    sum5=sum5/sum3
    write(15,*)'mean of N, m for the prior',sum4,sum5
    sum6=0.0
    do i=1,n
        do k=1,n
            sum6=sum6+(aN(k)*aN(k)*pprior(i,k))
        enddo
    enddo
    sum6=(sum6/sum3)-(sum4*sum4)
    sum7=0.0
    do i=1,n
        do k=1,n
            sum7=sum7+(am(i)*am(i)*pprior(i,k))
        enddo
    enddo
    sum7=(sum7/sum3)-(sum5*sum5)
    sum8=0.0
    do i=1,n

```

```

do k=1,n
sum8=sum8+(aN(k)*am(i)*pprior(i,k))
enddo
enddo
sum8=(sum8/sum3)-(sum4*sum5)
write(15,*)'covariance, cov(n,n),cov(m,m), cov(n,m) for the prior'
write(15,*)sum6,sum7,sum8
c*** calculating Mean and Covariance of the Posterior using the numerical method****
sum33=0.0
do i=1,n
do k=1,n
sum33=sum33+(ppost(i,k))
enddo
enddo
sum44=0.0
do i=1,n
do k=1,n
sum44=sum44+(aN(k)*ppost(i,k))
enddo
enddo
sum44=sum44/sum33
sum55=0.0
do i=1,n
do k=1,n
sum55=sum55+(am(i)*ppost(i,k))
enddo
enddo
sum55=sum55/sum33
write(15,*)'mean of N, m for the posterior',sum44,sum55
sum66=0.0
do i=1,n
do k=1,n
sum66=sum66+(aN(k)*aN(k)*ppost(i,k))
enddo
enddo
sum66=(sum66/sum33)-(sum44*sum44)
sum77=0.0
do i=1,n
do k=1,n
sum77=sum77+(am(i)*am(i)*ppost(i,k))
enddo
enddo
sum77=(sum77/sum33)-(sum55*sum55)
sum88=0.0

```

```

do i=1,n
  do k=1,n
    sum88=sum88+(aN(k)*am(i)*ppost(i,k))
  enddo
enddo
sum88=(sum88/sum33)-(sum44*sum55)
write(15,*)'cov(n,n),cov(m,m),cov(n,m) for the posterior'
write(15,*)sum66,sum77,sum88
ELSEIF(i_method.eq.2)then
c*****Calculating Mean and Covariance of the Prior using the numerical form*****
sum3=0.0
do i=1,n
  do k=1,n
    sum3=sum3+(pprior(i,k))
  enddo
enddo
sum4=0.0
do i=1,n
  do k=1,n
    sum4=sum4+(aN(k)*pprior(i,k))
  enddo
enddo
sum4=sum4/sum3
sum5=0.0
do i=1,n
  do k=1,n
    sum5=sum5+(am(i)*pprior(i,k))
  enddo
enddo
sum5=sum5/sum3
sum6=0.0
do i=1,n
  do k=1,n
    sum6=sum6+(aN(k)*aN(k)*pprior(i,k))
  enddo
enddo
sum6=(sum6/sum3)-(sum4*sum4)
sum7=0.0
do i=1,n
  do k=1,n
    sum7=sum7+(am(i)*am(i)*pprior(i,k))
  enddo
enddo
sum7=(sum7/sum3)-(sum5*sum5)

```

```

sum8=0.0
do i=1,n
  do k=1,n
    sum8=sum8+(aN(k)*am(i)*pprior(i,k))
  enddo
enddo
sum8=(sum8/sum3)-(sum4*sum5)
c***** getting sensivity Matrix at the MAP *****
  do j=1,nd
c***** calling subroutine iterate to use Newton method to get g(m) at MAP *****
    Call iterate(imax,kmax,j,aNmax,amax,aNp(j),Rp(j),Boi,Bgi,Rsi,
& g(j),dfpdpmax)
    write(13,*)j,g(j),dfpdpmax
    Call Sensivity(m,nd,j,g(j),dfpdpmax,aNmax,amax,Boi,Bgi,Rsi,
& Gsen(j,1),Gsen(j,2))
  enddo
c***** writing sensitivity *****
  do j=1,nd
    write(9,*)(Gsen(j,k), k=1,m)
  enddo
c***** form the matrix Cd^-1 in array Cd *****
  do i=1,nd
    do j=1,nd
      cd(i,j)=0.0
      If(i.eq.j)then
        cd(i,j)=1/(sdd**2.0)
      endif
    enddo
  enddo
c***** form the matrix Cm^-1 in array Cm *****
  do i=1,m
    do j=1,m
      Cm(i,j)=sum8
      If(i.eq.j)then
        if (i.eq.1) then
          Cm(i,j)=1/sum6
        else
          Cm(i,j)=1/sum7
        endif
      endif
    enddo
  enddo
c***** from matrix G^T at the MAP in array GsT *****
  do i=1,m

```



```

        do j=1,nd
        Gt(i,j)=Gsen(j,i)
        enddo
    enddo
c***** form the matrix (Cd^-1 * G) in array CdGs *****
    do i=1,nd
        do j=1,m
            sum1=0.0
            do k=1,nd
                sum1=sum1+(cd(i,k)*Gsen(k,j))
            enddo
            CdGs(i,j)=sum1
        enddo
    enddo
c***** form the matrix G^T * CdGs in array GtCdGs *****
    do i=1,m
        do j=1,m
            sum2=0.0
            do k=1,nd
                sum2=sum2+(Gt(i,k)*CdGs(k,j))
            enddo
            GtCdGs(i,j)=sum2
        enddo
    enddo
c***** form the matrix G^T * Cd^-1 * G + Cm^-1 in array Cmapinv *****
    do i=1,m
        do j=1,m
            Cmapinv(i,j)=GtCdGs(i,j)+Cm(i,j)
        enddo
    enddo
c***** write the matrix Cmapinv which is the Hessian *****
    do i=1,m
        write(11,*)(Cmapinv(i,j),j=1,m)
    enddo
    Close(11)
c**** call the subroutine matrixinversion to get the invese of the matrix Cmapinv ****
    CALL matrixinversion
c***** saving the inverse of the matrix Cmapinv in array Cmap *****
    open(12,file='Cmap.dat')
    do i=1,m
        read(12,*)(cmap(i,j), j=1,m)
    enddo
c***** writing the inverse of the matrix Cmapinv *****
    do i=1,m

```

```

write(17,*)(cmap(i,j), j=1,m)
enddo
endif
stop
END
c*****End Calculation*****

c*****
c This subroutine used to setup the prior pdf
c*****
Subroutine prpdf(n,m,j,aNavg,amavg,aN,am,Prm1,Prm2)
implicit double precision(a-h,o-z)
open(24,file = 'priormatrix.dat')
Prm1=aN-aNavg
Prm2=am-amavg
write(24,*)Prm1,Prm2
Return
End
c*****
c This subroutine used to calculate g(m) by using Newton Method
c*****
Subroutine iterate(i,k,j,aN,am,aNp,Rp,Boi,Bgi,Rsi,g,dfpdp)
implicit double precision(a-h,o-z)
open(4,file = 'iterate_results.dat')
open(7,file = 'check_iterate.dat')
write(7,*) aN,am,aNp,Rp,Boi,Bgi,Rsi,g
n=1
g=3200.0
2 Bo=(7.0*(10.0**(-5.0))*g)+1.0145
Bg=2.5965*(g**(-0.9867))
Rs=(0.1665*g)-48.638
F=aNp*(Bo+((Rp-Rs)*Bg))
Eo=(Bo-Boi)+((Rsi-Rs)*Bg)
Eg=Boi*((Bg/Bgi)-1.0)
fp=(F-(aN*(Eo+(am*Eg))))
dbo=7.0*(10.0**(-5.0))
dbg=-2.5965*0.9867*(g**(-1.9867))
drs=0.1665
dfdp=aNp*(dbo+(Rp*dbg)-(Bg*drs)-(Rs*dbg))
dEodp=dBo+(Rsi*dbg)-(drs*Bg)-(Rs*dbg)
dEgdp=(Boi/Bgi)*dbg
dfpdp=(dfdp-(aN*dEodp)-(aN*am*dEgdp))
g1=g-(fp/dfpdp)

```

```

        if(g1.lt.0.0.or.g1.gt.3330.0)then
            g=g1
        goto 3
    endif
    Bo=(7.0*(10.0**(-5.0))*g1)+1.0145
        Bg=2.5965*(g1**(-0.9867))
        Rs=(0.1665*g1)-48.638
        F=aNp*(Bo+((Rp-Rs)*Bg))
        Eo=(Bo-Boi)+((Rsi-Rs)*Bg)
    Eg=Boi*((Bg/Bgi)-1.0)
        fp=(F-(aN*(Eo+(am*Eg))))
        if(abs(fp).le.0.0001)then
            g=g1
            goto 1
        else
            g=g1
            n=n+1
            If(n.eq.100) then
                write(*,*)'No convergence'
            stop
            else
                goto 2
            endif
        endif
    endif
1      write(4,*)i,j,k,g,g1,n,dfpdp
3      Return
    end
c*****
c  This subroutine calculates the sensivity coeffecient at each data point analytically
c*****
    Subroutine Sensivity(m,nd,j,g,dfpdpmax,aNmax,amax,Boi,Bgi,Rsi,
*   Gs1,Gs2)
    implicit double precision(a-h,o-z)
c    dimension Gs(nd,m)
    open(10,file = 'check_sensitivity.dat')
    Bo=(7*(10**(-5))*g)+1.0145
        Bg=2.5965*(g**(-0.9867))
        Rs=(0.1665*g)-48.638
    Eo=(Bo-Boi)+((Rsi-Rs)*Bg)
    Eg=Boi*((Bg/Bgi)-1)
    dfpdN=-(Eo+(amax*Eg))
    dfpdm=-aNmax*Eg
    dgdN=(1/dfpdpmax)*dfpdN
        dgdM=(1/dfpdpmax)*dfpdm

```

```

c   dlngdN=0.4343*(1/g)*dgdN
c   dlngdm=0.4343*(1/g)*dgdM
      Gs1=dgdN
      Gs2=dgdM
      write(10,*)Gs1,Gs2,g,dfpdpmax
      Return
      End
c*****
c   Subroutine to get the inverse of any matrix of dimension np x np
c*****
      Subroutine matrixinversion
      implicit Double Precision(a-h,o-z)
c   PARAMETER(np=15*15*2,n=15*15*2)
      PARAMETER(np=2,n=2)
      dimension a(np,np), y(np,np), indx(np)
      open(11,file='Cmapinv.dat')
      open(12,file='Cmap.dat')
      do i=1,np
        read(11,*)(a(i,j),j=1,np)
      enddo
      do i=1,n
        do j=1,n
          y(i,j)=0.
        end do
        y(i,i)=1.
      end do
      call ludcmp(a,n,np,indx,d)
      do j=1,n
        call lubksb(a,n,np,indx,y(1,j))
c   Note that FORTRAN stores two-dimensional matrices by columns,
c   so y(1,j) is the address of the jth column of y.
      end do
      do i=1,n
        write(12,*)(y(i,j), j=1,n)
      enddo
      close (12)
      Return
      END
c*****
c   Subroutine to get the inverse of prior matrix np x np
c   Modified By Chile Ogele ... February 2005
c*****
      Subroutine prmxinversion
      implicit Double Precision(a-h,o-z)

```

```

PARAMETER(np=2,n=2)
  dimension a(np,np), y(np,np), indx(np)
  open(21,file='Cprmx.dat')
  open(22,file='Cprmxinv.dat')
do i=1,np
  read(21,*)(a(i,j),j=1,np)
  enddo
do i=1,n
  do j=1,n
    y(i,j)=0.
  end do
  y(i,i)=1.
end do
call ludcmp(a,n,np,indx,d)
do j=1,n
  call lubksb(a,n,np,indx,y(1,j))
end do
do i=1,n
  write(22,*)(y(i,j), j=1,n)
  enddo
close (22)
Return
END
c*****
SUBROUTINE ludcmp(a,n,np,indx,d)
c*****
  implicit Double Precision(a-h,o-z)
  PARAMETER (NMAX=100000,TINY=1.0d-20)
  dimension indx(n),a(np,np),vv(nmax)
  d=1.
  do 12 i=1,n
    aamax=0.
    do 11 j=1,n
      if (abs(a(i,j)).gt.aamax) aamax=abs(a(i,j))
11  continue
      if (aamax.eq.0.) pause 'singular matrix in ludcmp'
      vv(i)=1./aamax
12  continue
    do 19 j=1,n
      do 14 i=1,j-1
        sum=a(i,j)
        do 13 k=1,i-1
          sum=sum-a(i,k)*a(k,j)
13  continue

```

```

    a(i,j)=sum
14  continue
    aamax=0.
    do 16 i=j,n
        sum=a(i,j)
        do 15 k=1,j-1
            sum=sum-a(i,k)*a(k,j)
15  continue
    a(i,j)=sum
    dum=vv(i)*abs(sum)
    if (dum.ge.aamax) then
        imax=i
        aamax=dum
    endif
16  continue
    if (j.ne.imax)then
        do 17 k=1,n
            dum=a(imax,k)
            a(imax,k)=a(j,k)
            a(j,k)=dum
17  continue
    d=-d
    vv(imax)=vv(j)
    endif
    indx(j)=imax
    if(a(j,j).eq.0.)a(j,j)=TINY
    if(j.ne.n)then
        dum=1.0d0/a(j,j)
        do 18 i=j+1,n
            a(i,j)=a(i,j)*dum
18  continue
    endif
19  continue
    return
    END
c*****
    SUBROUTINE lubksb(a,n,np,indx,b)
c*****
    implicit Double Precision(a-h,o-z)
    dimension indx(n),a(np,np),b(n)
    ii=0
c    write(*,*)'lub,n,np,b',n,np
    do i=1,n
c    write(*,*)'b',b(i)

```

```
    enddo
    do 12 i=1,n
      ll=indx(i)
      sum=b(ll)
      b(ll)=b(i)
      if (ii.ne.0)then
        do 11 j=ii,i-1
          sum=sum-a(i,j)*b(j)
11      continue
        else if (sum.ne.0.) then
          ii=i
        endif
        b(i)=sum
12      continue
      do 14 i=n,1,-1
        sum=b(i)
        do 13 j=i+1,n
          sum=sum-a(i,j)*b(j)
13      continue
        b(i)=sum/a(i,i)
14      continue
      return
    END
```

APPENDIX B
MODIFIED SUBROUTINE FOR EXAMPLE 2

```

c*****
c      This modifies the subroutine used to calculate g(m) for Example 2 because g(m)
c      depends on the equation of each PVT variable as a function of pressure.
c*****
      Subroutine iterate(i,k,j,aN,am,aNp,Rp,Boi,Bgi,Rsi,g,dfpdp)
      implicit double precision(a-h,o-z)
      open(4,file = 'iterate_results.dat')
      open(7,file = 'check_iterate.dat')
      write(7,*) aN,am,aNp,Rp,Boi,Bgi,Rsi,g
      n=1
      g=1620.0
2     Bo=1.123*10.**((0.00006986*g)
      Bg=0.0079803-0.0000061666*g+0.000000001509*(g**2.)
      Rs=294.4*10.**((0.0002715*g)
      F=aNp*(Bo+((Rp-Rs)*Bg))
      Eo=(Bo-Boi)+((Rsi-Rs)*Bg)
      Eg=Boi*((Bg/Bgi)-1.0)
      fp=(F-(aN*(Eo+(am*Eg))))
      dbo=0.000181*10.**((0.00006986*g)
      dbg=0.000000003018*g-0.0000061666
      drs=0.184045*10.**((0.0002715*g)
      dfdp=aNp*(dbo+(Rp*dbg)-(Bg*drs)-(Rs*dbg))
      dEodp=dbo+(Rsi*dbg)-(drs*Bg)-(Rs*dbg)
      dEgdp=(Boi/Bgi)*dbg
      dfpdp=(dfdp-(aN*dEodp)-(aN*am*dEgdp))
      g1=g-(fp/dfpdp)

      if(g1.lt.0.0.or.g1.gt.16400.0)then
      g=g1
      goto 3
      endif
      Bo=1.123*10.**((0.00006986*g)
      Bg=0.0079803-0.0000061666*g+0.000000001509*(g**2.)
      Rs=294.4*10.**((0.0002715*g)
      F=aNp*(Bo+((Rp-Rs)*Bg))
      Eo=(Bo-Boi)+((Rsi-Rs)*Bg)
      Eg=Boi*((Bg/Bgi)-1.0)
      fp=(F-(aN*(Eo+(am*Eg))))
      if(abs(fp).le.0.0001)then

```



```

        g=g1
        goto 1
    else
        g=g1
        n=n+1
        If(n.eq.100) then
            write(*,*)'No convergence'
        stop
        else
            goto 2
        endif
    endif
1    write(4,*)i,j,k,g,g1,n,dfpdp
3    Return
    end
c*****
c  This subroutine calculates the sensivity coefferent at each data point analytically
c*****
Subroutine Sensivity(m,nd,j,g,dfpdpmax,aNmax,amax,Boi,Bgi,Rsi,
*   Gs1,Gs2)
implicit double precision(a-h,o-z)
c    dimension Gs(nd,m)
open(10,file = 'check_sensivity.dat')
Bo=1.123*10.**(0.00006986*g)
Bg=0.0079803-0.0000061666*g+0.000000001509*(g**2.)
Rs=294.4*10.**(0.0002715*g)
Eo=(Bo-Boi)+((Rsi-Rs)*Bg)
Eg=Boi*((Bg/Bgi)-1)
dfpdN=-(Eo+(amax*Eg))
dfpdm=-aNmax*Eg
dgdN=(1/dfpdpmax)*dfpdN
dgdM=(1/dfpdpmax)*dfpdm
c  dlngdN=0.4343*(1/g)*dgdN
c  dlngdm=0.4343*(1/g)*dgdM
Gs1=dgdN
Gs2=dgdM
write(10,*)Gs1,Gs2,g,dfpdpmax
Return
End

```

VITA

Name : Chile Ogele

Permanent Address : Chevron Nigeria Mail Pouch
P.O. Box 6046
San Ramon, CA 94583

Email : chileogele@msn.com
chileogele@chevron.com

Education : B.Eng., Petroleum Engineering, University of Port Harcourt, 1991
M.Eng., Petroleum Engineering, University of Port Harcourt,
1995
M.S., Petroleum Engineering, Texas A&M University, 2005